Ad Hoc Networks 59 (2017) 116–133

Contents lists available at ScienceDirect

Ad Hoc Networks

journal homepage: www.elsevier.com/locate/adhoc

# Real-time link quality estimation for industrial wireless sensor networks using dedicated nodes

Ruan D. Gomes[a,b,*], Diego V. Queiroz[c], Abel C. Lima Filho[d], Iguatemi E. Fonseca[c], Marcelo S. Alencar[b]

[a] Informatics Coordination, Federal Institute of Paraíba, Campus Guarabira, Paraíba, Brazil
[b] Post-Graduate Program in Electrical Engineering, Federal University of Campina Grande, Campina Grande, Brazil
[c] Informatics Center, Federal University of Paraíba, João Pessoa, Brazil
[d] Mechanical Engineering Department, Federal University of Paraíba, João Pessoa, Brazil

ARTICLE INFO

*Article history:*
Received 24 August 2016
Revised 24 February 2017
Accepted 27 February 2017
Available online 28 February 2017

*Keywords:*
Industrial wireless sensor networks
Link quality estimation
Adaptive protocols

ABSTRACT

Adaptive mechanisms, such as dynamic channel allocation or adaptive routing, are used to deal with the variations in the link quality of Wireless Sensor Networks (WSN). In both cases, the first step is to estimate the link quality, so that the network nodes can decide if a channel or route change is needed. This paper proposes a Link Quality Estimator (LQE) for Industrial WSN, and a new type of node, the LQE node, that estimates the link quality in real-time, using the Received Signal Strength Indication (RSSI), and information obtained from received data packets. The proposed LQE is capable of capturing the effects of multipath, interference, and link asymmetry. Experiments were performed in a real industrial environment using IEEE 802.15.4 radios, and models were developed to allow the use of RSSI samples to proper estimate the link quality. A comparison was performed with a state-of-the-art LQE, the Opt-FLQE, and the results showed that the proposed estimator is more accurate and reactive for the type of environment in study. Different from other LQEs in literature, in the proposed LQE the sensor nodes do not need to send broadcast probe packets. Besides, using the LQE node, the other nodes of the WSN do not need to stop their operation to monitor the link quality.



## 1. Introduction

The use of Wireless Sensor Networks (WSN) to implement monitoring and control systems in industrial environments has some advantages when compared with the use of wired networks, such as low cost and high flexibility. Some applications were proposed in literature, such as motor monitoring [1], temperature monitoring [2], and aperiodic wireless control systems [3]. However, it is necessary to deal with typical problems of wireless networks, such as electromagnetic interference [1], and high attenuation, due to the presence of many objects and obstructions [4]. Many industrial environments also present characteristics that make the wireless channel non-stationary, for long time periods, which can cause abrupt changes in the characteristics of the channel over time [5].

It is possible to deal with these problems using mechanisms that allow the network to self-adapt to the variations that occur in the link quality over time, such as adaptive routing [6] or Dynamic Channel Allocation (DCA) [7], in which the WSN nodes change the route or the channel when the quality decreases. The IEEE 802.15.4 standard, which is the usual communication standard for WSN, defines sixteen channels in the 2.4 GHz band, and the characteristics of the communication medium can be different for different channels [8]. Even for standardized devices, that use channel hopping, such as the WirelessHART and ISA100 [9], the use of DCA mechanisms can be advantageous to properly configure the blacklist, in order to dynamically modify the channels that are considered in the channel hopping mechanism. To implement these adaptive protocols, a Link Quality Estimator (LQE) is necessary to provide information about the quality of the links to the network nodes.

This paper proposes a novel LQE and a new architecture for industrial WSN. The use of dedicated nodes (the LQE nodes) to monitor the link quality in industrial WSN is considered. Using the LQE node, the Received Signal Strength Indication (RSSI) can be used in a more effective way, since raw values of RSSI are not enough to properly estimate the quality of the wireless channel, but with

* Corresponding author.
*E-mail addresses:* ruan.gomes@ifpb.edu.br, ruandgomes@gmail.com (R.D. Gomes), diego@sti.ufpb.br (D.V. Queiroz), abel@les.ufpb.br (A.C. Lima Filho), iguatemi@ci.ufpb.br (I.E. Fonseca), malencar@dee.ufcg.edu.br (M.S. Alencar).

http://dx.doi.org/10.1016/j.adhoc.2017.02.007
1570-8705/

a more detailed analysis of several values of RSSI it is possible to identify the problems that affect the channel quality.

Two main challenges are addressed in this paper. The first one is the development of metrics to capture all the aspects of the channel that affect the link quality and its dynamics, such as fading, shadowing, interference, and link asymmetry. It is necessary to find a good trade-off between the stability and reactivity, to estimate the link quality accurately, even with the small and rapid variations in the channel quality due to the multipath fading. On the other hand, it is necessary to rapidly identify abrupt and persistent changes in the link quality.

The second one is the design and implementation of a LQE that allows to monitor, in real-time, the quality of various links, without causing overhead on the sensor nodes, or on the network, especially on the end nodes, which present additional resource constraints. Thus, the models developed to implement the proposed LQE use only information obtained at the receiver side, and no extra traffic is generated in the network. Besides, the LQE must have low computational complexity in order to run on low-cost microcontrollers. Even considering these restrictions, the LQE must be capable of evaluating the quality of the link, in both directions, and identify interference problems.

Different from other LQEs [10–14], the proposed LQE does not generate extra traffic through the use of probe packets or redundancy in the data packets, neither performs processing on the transmitter. This approach allows real-time estimation using the LQE node, which can process many values of RSSI, and information obtained from received data packets, while the other nodes of the WSN remain operating normally, which incurs in a low overhead. A comparison was made with the Opt-FLQE [13] estimator, which is a LQE based on fuzzy logic. The results showed that the proposed estimator is more accurate and reactive for the type of environment in study.

The main contributions of this paper are:

- The realization of a comprehensive set of experiments in a real industrial environment using IEEE 802.15.4 radios to obtain insights on the implementation of the LQE node;
- The development of models to estimate the link quality in both directions and the influence of interference, using samples of RSSI and information obtained from received data packets;
- The design and implementation of a new type of node, the LQE node, and a novel LQE, to estimate the link quality in real-time;
- The validation of the proposed estimator through experiments in a real industrial environment.

## 2. Background information

### 2.1. The wireless channel in industrial environments

The industrial environment usually contains metallic and mobile objects, such as robots, cars and people. This influences both the large-scale and small-scale fading. The power of the received signals depends on the transmission power, the antennas gains, the distance between transmitter and receiver and the effects caused by the environment. Even with the same values for the aforementioned parameters, there is a variation in the mean received power, depending on the place where the measurement is performed, which is known as log-normal shadowing. The log-normal shadowing model has been used to model the large-scale path loss and shadowing in industrial environments [4].

Besides path loss and shadowing, it is also necessary to analyze the small-scale channel fading due to rapid changes in the multipath profile of the environment, which is caused by the movement of objects around the receiver and transmitter. Experiments demonstrated that, in industrial environments, the temporal attenuation follows a Rice distribution. In industrial environments the K factor of the Rice distribution has a high value. For the experiments described in [4], in industrial environments, K presented values between 4 dB and 19 dB, while in office environments, values between −12 dB and −6 dB were reported, as discussed in [4]. This can be explained by the open nature of industrial buildings and the large amount of reflective materials. Thus, there are many time-invariant rays and only a small part of the multipath profile is affected by moving objects.

A study on the properties of the error in bit and symbol-level, in industrial environments, was described in [15]. For environments with multipath fading, the bit errors are uniformly distributed inside the corrupted packets, and the channel memory is only four bits long. The use of forward error correction was proposed. However, most of packets in the experiments were lost in air, in scenarios with multipath fading. Thus, to achieve good quality, it is also necessary to pick channels or routes that suffer less with the multipath fading.

The wireless channel can be modeled as wide-sense stationary for a short period of time. However, the channel's properties can change significantly in a period of a few hours, due to changes in the topology of the environment. This changes are not taken into account by the usual fading distributions [16].

A characterization of the wireless channel in an industry was performed for a long time period (20 h) in [17]. The results showed that the Rice distribution only fits the received power for small periods of time, in which the mean value of the received power remains constant. However, abrupt changes in the channel characteristics can occur when the channel is analyzed for a long term, and differences on the mean value of the received power are observed, although the transmitter and receiver remain static. For example, in the experiment described in [17], the received power varied around −55 dBm during 7 h, and after this period the mean value of the received power changed abruptly to −46 dBm. An experiment described in [18] also presented similar behavior.

A composite distribution has been described to capture both shadowing, and fading for the long term. The model is called Nakagami-m/Log-normal. The parameter of the Nakagami-m distribution defines the level of fading, and the parameters of the log-normal distribution define the effects of shadowing [5].

#### 2.1.1. Power delay profile and coherence bandwidth

Some papers have described experiments to identify the Root-Mean-Square (RMS) delay spread in industrial environments [19,20]. The RMS delay spread gives an indication of the level of multipath encountered during the signal transmission, and is calculated from the power delay profile of a measured signal [20].

Reflective industrial environments present many multipath components, which lead to a high value of RMS delay spread. For example, in the experiments described in [19], in the 2.4 GHz band, the RMS delay spread was 294.19 ns. As the radios used in WSN have relatively low symbol rate, the inter-symbol interference may not be a problem for WSN in indoor environments.

The coherence bandwidth is the frequency interval ($\Delta f$) in which the frequency components are correlated, and can be defined according to $\Delta f \approx 1/\alpha\tau_{RMS}$, in which $\tau_{RMS}$ is the RMS delay spread in seconds, and $\alpha$ is a factor that can vary according to the shape of the power delay profile [21]. Considering $\tau_{RMS} = 294.19$ ns for an industrial environment [19], and considering $\alpha = 5$ (correlation between frequencies larger than 90%), $\Delta f \approx 10^9/(5 \times 294.19) \approx 680$ kHz.

The IEEE 802.15.4 standard defines sixteen channels in the 2.4 GHz band, with 2 MHz of bandwidth, and channel spacing of 5 MHz. Thus, the channels are highly uncorrelated. Experiments described in [22] have found that changing the communication channel can lead up to 30 dB difference in the received power, in

an office environment. Varga et al. [8] performed experiments for a short range, in an environment without multipath, and with line-of-sight. In that experiment, differences up to 10 dB were observed for some channels. Experiments described in [23], in an office environment, showed that for distances larger than 6.5 m between transmitter and receiver, even the adjacent channels are uncorrelated. This difference may be larger in channels with high RMS delay spread, as can occur in many industrial environments.

There are three solutions to deal with the link quality variations in WSN, that is, modify the position of the node, change the route, or change the channel. The first two solutions are not applicable in many cases, while the third solution is always possible. Experiments described in [24] showed that for multi-hop networks, multi-channel communication and adaptive routing present similar performance for dense networks, but for sparse networks multi-channel communication presents a better performance, since in this scenario adaptive routing present less flexibility. For networks with star topology, dynamic channel allocation may be the only alternative.

Although change the route or the position of a node can be useful to overcome fading and shadowing problems, in some cases these mechanisms cannot solve interference problems. The industrial WSNs usually are planned, and use a tree or star topology, with centralized or static routing decisions. When it is not possible to switch the route dynamically, switch the channel can improve the quality of a link.

### 2.2. Link quality estimation for WSN

Some LQE are based on physical layer information (hardware-based estimators), such as the Link Quality Indicator (LQI) and the RSSI, and other are based on information from upper layers (software-based estimators), such as the Packet Reception Rate (PRR) [25]. For industrial WSN the LQE needs to be accurate, and stable to avoid switch the channel or the route very frequently due to small and rapid variations, which would cause a high delay. On the other hand, the LQE needs to rapidly identify abrupt and persistent changes in the channel characteristics. Besides, the estimation needs to be performed without causing a high overheard in the nodes and on the network. The LQE proposed in this paper tries to satisfy these requirements.

#### 2.2.1. Hardware-based LQEs

The hardware-based LQEs do not demand computational resources from the sensor nodes, since the metric values are provided by the transceiver. However, using only the information provided by hardware-based estimators directly may not be sufficient, therefore some processing should be performed to extract useful information.

Each packet received by the IEEE 802.15.4 radios has values of RSSI and LQI associated to it. However, RSSI can be obtained regardless of the reception of a packet. Any device that generates interference in the frequency range of the channel can influence the RSSI value. The LQI can only be measured during the reception of a packet, since the measurement is based on the analysis of the initial symbols of the received packets. Thus, when the network experiences a high Packet Error Rate (PER), this metric can overestimate the link quality, since it does not consider the lost packets [26]. Besides, as the implementation of LQI is vendor-specific [27], it is difficult to develop a general solution using this metric. Raw values or averaged values of small samples of RSSI have a low correlation with the PRR in very reflective environments [25,26], due to the random variation of the energy level in such environments.

Some works used the RSSI or LQI to estimate the channel quality. Noda et al. [28] proposed two metrics to assess the quality of the channel based on channel vacancies. Although this metric can identify channels that are less affected by sources of impulsive noise, it may also present problems to estimate the channel quality in the presence of multipath fading. Zacharias et al. [29] proposed an algorithm to identify the presence of Wi-Fi networks, Bluetooth networks or microwave ovens, using RSSI samples. The analysis is based on the periodicity of interference sources. It also consider only interference problems.

Jindong et al. [30] proposed a metric to estimate the channel quality using RSSI and LQI. This metric showed good correlation with the PER in experiments and a smaller variance in comparison with the use of only RSSI or LQI. In the presence of sources of interference and multipath, this approach may provide erroneous results, since it uses raw values obtained from received packets. Bildea et al. [31] studied the correlation between RSSI, LQI and PRR. The RSSI was not a very accurate estimator of PRR in the experiments. Thus, the work has focused on the utilization of LQI. However, the metrics based on LQI may overestimate the channel quality in scenarios with impulsive noise, since the LQI of lost packets is not considered.

Eskola et al. [32] proposed a classifier to identify disturbances in the wireless channel, which is capable to identify if a channel has line-of-sight or not, and if there is external interference. However, the proposed technique is only capable of identifying the existence of disturbances, but does not provide any metric, that could be used by protocols to dynamically optimize the network performance. In addition, the analysis is made in modulation level, using a software-defined radio, which is impractical to be done with off-the-shelf WSN radios.

#### 2.2.2. Software-based LQEs

The software-based LQEs use information obtained from upper layers, such as the PRR, and the Required Number of Packet Transmissions (RNP). The use of metrics based on PRR allows a good estimation for links with a very high or a very low quality, but present some problems in intermediate links. When retransmission is used, the metrics based on PRR overestimate the link quality, since they do not consider the number of transmission attempts before a successful reception. The metrics based on RNP estimate the required number of packet transmissions until a successful reception. The Expected Transmission Count (ETX) and Four-Bit (FB) are examples of RNP-based estimators.

The ETX [10] is a receiver-initiated estimator, which considers link asymmetry by estimating the PRR in both directions, according to $e(w) = 1/(p_b \times p_f)$, in which $e(w)$ is the value of ETX calculated using a set of $w$ received packets in each direction, $p_b$ is the PRR of the backward link, and $p_f$ is the PRR of the forward link. Probe broadcast packets are used to calculate the $p_b$ and $p_f$, which causes overhead in all nodes of the network and also generates extra traffic. The correlation between ETX, RSSI, and LQI was verified in [33], for an indoor office environment, and for different outdoor environments, using raw values of RSSI and LQI. In the experiments, no significant correlation was found between the metrics. As discussed in Section 2.2.1, RAW values of RSSI and LQI are not sufficient to proper estimate the link quality. The two LQE strategies (one passive and one active) implemented in the IPv6 Routing Protocol for Low power and Lossy Networks (RPL) were evaluated in [34]. When using active estimation, probe packets are sent to calculate the ETX. In the experiments described in [34] the performance of the estimator was better when using active estimation. However, this approach imposes an overhead in the sensor nodes and on the network.

The FB implements a hybrid active/passive, and sender-initiated estimator [11], that uses four bits of information. The first bit is obtained from the physical layer, to identify the quality of the channel in a received packet. The second bit (ACK bit) is obtained from the link layer, and considers forward and backward links. The other

two bits are obtained from the network layer, and are useful for route decisions [25].

The ACK bit is determined using data packets and probe broadcast packets, that are combined to compute an estimate of the ETX. The value of ETX calculated using broadcast packets ($e_b$), is computed using $e_b = 1/p_f(w_b, \alpha)$ , in which $p_f(w_b, \alpha)$ is an estimation of the PRR, using an Exponentially Weighted Moving Average (EWMA) filter with history control factor $\alpha$, and using a window with $w_b$ probe packets.

The value of ETX calculated using data packets ($e_d$) is computed using $e_d = w_d/a$, in which $a$ is the number of ACK packets received for each $w_d$ transmitted data packets. If $a$ is equal to zero, $e_d$ is equal to the number of transmissions after the last ACK received. To estimate the overall ETX, the values of $e_b$ and $e_d$ are combined using an EWMA filter. This estimator generates extra traffic due to the probe packets, and most of the overhead is on the transmitter.

A simulation study was performed to compare five different LQEs (PRR, RNP, WMEWMA, ETX, and FB) on the collection tree routing protocol for smart-grid environments in [35]. In the simulations described in the paper, ETX and FB presented a better performance in harsh smart grid environments, since only ETX and FB consider the link asymmetry among the evaluated LQEs.

Most existing LQEs are not sufficiently accurate because they use only a single metric (e.g., RSSI or PRR), that provides just a partial characterization of the link [25]. Some LQEs that use fuzzy logic to combine different aspects of the link quality were proposed in the literature. A fuzzy logic based link quality indicator (FLI) was proposed in [36]. The FLI uses the PRR, the coefficient of variance of PRR, and a metric to assess the burstiness of packet loss, to estimate link quality. The metrics are calculated using the number of received and lost ACK packets. The FLI outperformed FB in the experiments described in the paper. In the FLI the overhead is restricted to the transmitter, as well is the case in FB.

The F-LQE [12] is a receiver-initiated estimator based on fuzzy logic. Four different aspects of the link are used to obtain a holistic characterization, that is: packet delivery (SPRR), stability (SF), asymmetry (ASL), and channel quality (SNR or LQI). The SPRR is the PRR filtered using an EWMA filter. The SF is the coefficient of variation of PRR. To assess the asymmetry of the link the PRR calculated in the neighbor nodes are used. The values of PRR in each node are calculated using probe broadcast packets, and are transmitted together with the data packets. To calculate the SNR, one value of RSSI is sampled from a received packet, and other value of RSSI is sampled after the packet reception, to obtain the noise floor. The SNR is then calculated subtracting these two values. In the experiments described in [12], the F-LQE outperformed ETX and FB.

The Opt-FLQE [13] is a modification of the F-LQE to improve the reactivity and reduce the computational complexity. It does not use the SF, and to replace it, the Opt-FLQE uses a sender-side metric, the Smoothed RNP (SRNP). The values of SRNP calculated at the sender are transmitted together with the data packets to allow the receiver calculate the Opt-FLQE metric.

The four metrics considered in Opt-FLQE are combined using fuzzy logic to compute the quality of link $i$ as follows

$$\mu(i) = \beta \min(\mu_{SPRR}(i), \mu_{ASL}(i), \mu_{SRNP}(i), \mu_{SNR}(i)) + (1-\beta)\text{mean}(\mu_{SPRR}(i), \mu_{ASL}(i), \mu_{SRNP}(i), \mu_{SNR}(i)), \quad (1)$$

in which $\mu_{SPRR}(i)$, $\mu_{ASL}(i)$, $\mu_{SRNP}(i)$, and $\mu_{SNR}(i)$ are the membership functions of each metric, which provide a value between [0, 1], that indicates the extent to which the link is considered having high delivery rate, low asymmetry, low number of packet retransmissions, and high channel quality, respectively. In [13] $\beta = 0.6$ was used. All membership functions used in [12] and [13] are linear. The final values of Opt-FLQE are the value of $\mu(i)$ normalized to fit between 0 and 100, and smoothed using an EWMA filter. In [13] $\alpha = 0.9$ was used for the EWMA filter.

The performance analysis described in [13] showed that Opt-FLQE is more reactive than F-LQE, while still being more reliable for smart-grid environments. The Opt-FLQE was compared to the ETX and FB on the RPL routing protocol, for smart grid environments in [37]. In the evaluation described in the paper, the ASL was not considered, in order to reduce the computational complexity, since SNP and SPRR are sufficient to assess the asymmetry of the link. In the described simulations, the Opt-FLQE outperformed the ETX and the FB for all evaluated metrics.

Barac et al. [14] proposed the use of Forward Error Correction (FEC) to perform channel diagnostics for WSN in industrial environments. The proposed solution is called Lightweight Packet Error Discriminator (LPED), and uses only information obtained from received data packets, without using probe packets. As in the study described in [32], the LPED is capable of identifying fading or interference problems in the wireless channel, but does not provide any metric to assess the link quality in terms of a network performance indicator, such as the PRR or the RNP. The use of methods that identify only the presence of disturbances, using information obtained from a few packets, may lead the network to make changes in the routes or channels due to rapid variations in the quality of the channels, which can impairs the stability of the used protocol. It is important to differentiate small and rapid variations in the channel quality from abrupt and persistent variations.

The use of FEC can be useful also to recover some corrupted packets, but when good channels or routers are picked (which is also the goal of the use of LPED), the signal-to-noise ratio is increased, and then the use of FEC may not be advantageous. Using the solution proposed in the current paper, the use of FEC can also be used as a complement depending on the application, and the information provided by the LQE node can be used to decide when the use of FEC is necessary.

Even the LPED has a low computational complexity, the execution time in the worst case is 30 ms, which can cause a significant overhead in the nodes responsible to perform the calculations if the number of links being monitored increases. In the experiments described in [14] packets with 30 bytes or more were considered. However, for some industrial WSN, such as Low Latency Deterministic Networks (LLDN), the packets need to be significantly smaller (with only a few bytes) [38]. Besides, even considering that the decoding time is significantly higher than encoding time, as discussed in [15], the use of FEC can cause a significant overhead on the end nodes, since there is an increase in the size of the packets, which can cause a significant increase in the energy consumption. In the solution proposed in the current paper, no overhead is imposed on the end nodes, and there is no dependence on the size of the packets.

It may be difficult to integrate the software-based LQEs described in this section to TDMA-based industrial WSN, such as networks based on the standards WirelessHART, ISA100.11a, or IEEE 802.15.4e, due to the time constraints of these networks. In some cases, it may be difficult to allocate time-slots to perform link quality estimation or the transmission of probe packets. In addition, the time needed to estimate the link quality may be much higher than the size of the time-slots in the network. The time-slots in WirelessHART, and ISA100.11a networks, as well as in networks based on the Time Slotted Channel Hopping (TSCH) mode of the IEEE 802.15.4e standard, have 10 ms of duration (in ISA100.11a networks time-slots with up to 12 ms are also used) [39,40].

The Deterministic and Synchronous Multi-channel Extension (DSME) mode of the IEEE 802.15.4e standard is more flexible, and can use lower time-slots [40]. The LLDN mode of the IEEE 802.15.4e can use time-slots with sizes equal to approximately 1 ms [38]. Thus, the use of dedicated nodes, as proposed in the

current paper, is a possible solution to integrate real-time link quality estimation in many industrial WSN, even for those with strict time constraints.

It is worth to notice that the use of dedicated nodes to monitor link quality has not been taken into account in the cited articles. The use of large samples of RSSI to identify transmission effects and multipath problems in an industrial WSN was not considered. One disadvantage of most approaches discussed in this section is that they generate extra traffic, due to the probe packets. Besides, they cause overhead in all nodes of the network to compute the values of the metrics, including the transmitter, which usually is the end node of the WSN. The LPED does not use probe packets, but generates extra traffic due to the use of FEC and cause overhead in the end nodes of the network.

The advantage of LPED in comparison to the other software-based approaches discussed in this section is that it is possible to identify the type of the disturbance (fading or interference), which can help the protocols to make the best decision for each case. The disadvantage is that only one direction of the link is evaluated, which cannot be sufficient for protocols that use acknowledgment. The CSMA/CA protocol described in the IEEE 802.15.4 standard, and also the protocols described in other standards for industrial WSN consider the use of acknowledgment per packet, such as the WirelessHART, ISA100.11a, the TSCH and the DSME [39,40].

The solution proposed in the current paper is capable of evaluating the quality of the link, in both directions, and identify interference and multipath problems separately. With the use of dedicated nodes, no overhead is imposed in the WSN nodes, which allows the real-time link quality estimation even for WSN with strict time constraints, and for WSN that use acknowledgment per packet. The LQE proposed in this paper is compared to the Opt-FLQE [13] in an industrial environment in Section 5. The Opt-FLQE is the most recent work between the aforementioned papers, and is capable to estimate the quality of the links in both directions. Besides, it was developed to be suitable for smart grid applications, in harsh environments.

## 3. The LQE node

In addition to end nodes, routers, and sink nodes, this paper proposes a new type of node: the LQE node. The end nodes are responsible to acquire data from sensors, perform local processing, and transmit the information to the sink node. The transmission can occur directly, or indirectly using intermediate routers.

The LQE nodes estimate, in real-time, the quality of the links of the WSN, using a detailed analysis of the RSSI, while the other nodes remain operating normally. Raw values of RSSI or LQI are not enough to properly estimate the channel quality, but with a more detailed analysis of many values of RSSI it is possible to identify the problems that affect the channel quality. In this paper large samples of RSSI are considered to estimate the channel quality, regarding the influence of the multipath and interference. Besides, the number of duplicate packets received are also used to estimate the quality of the link, considering the asymmetry.

The LQE nodes can be associated to the nodes that receive data packets in the network, that is, the sink nodes and routers. However, when retransmission is used, the end nodes need to receive ACK packets. Besides, control packets may also be transmitted to the end nodes. In this case, the quality of packet reception also needs to be ensured for the end nodes. Thus, the estimator to be executed on the LQE node needs to consider the backward quality of the link.

In networks with a star topology, it is necessary to have only LQE nodes integrated to the sink nodes. Ideally the LQE node has to be build integrated in the same PCB of the node in which it is associated, with the transceivers of the two nodes positioned very close to each other. Thus, problems that can arise due to the spatial variation in the link quality can be mitigated, since the multipath profile and the effect of interference sources varies with the location. Experiments described in [23] found a coherence length of 5.5 cm between IEEE 802.15.4 transceivers, in which two antennas separated with this distance can be considered completely uncorrelated.

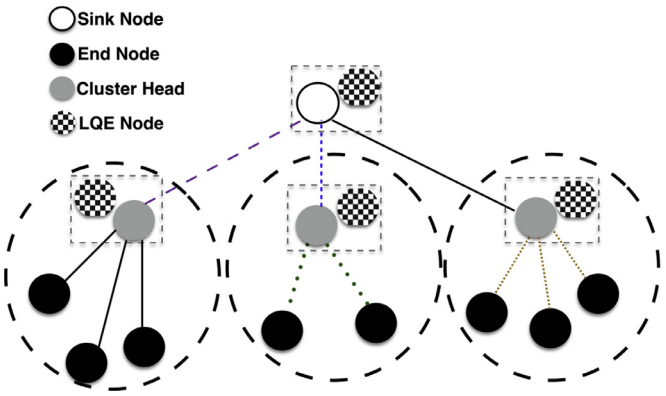


**Fig. 1.** A three layer topology for WSN with LQE nodes.

Fig. 1 shows a possible network topology that can be used to implement an industrial WSN based on the proposed architecture. In this topology the end nodes are clustered, and each cluster can operate in a different channel [41]. The end nodes transmit packets to an intermediate node (called Cluster Head – CH) that routes the packets to the sink node. Some standards designed for WSN considers the use of star or tree topology, such as the IEEE 802.15.4e standard [40], which has a focus on industrial applications.

However, the proposed solution can also be used to implement networks that use redundant routes. In this case, a given end node can connect simultaneously to multiple CH nodes, and the quality of each link can also be monitored simultaneously by the LQE nodes integrated to the CH nodes. The LQE node can also be used to help in the resynchronization process after a channel switch. Since this paper focuses on link quality estimation, the details of the implementation of protocols that can use the estimator, such as adaptive routing protocols or multi-channel protocols are beyond the scope of this paper.

The addition of the LQE nodes increases the cost slightly, since they are employed associated to some nodes of the network. For example, in small networks, with a star topology, it is necessary to employ only one LQE node associated to the sink node. There are off-the-shelf IEEE 802.15.4 transceivers that costs less than US$ 10.00 (in large scale acquisition the cost is even smaller). The LQE nodes are composed of a low-cost micro-controller and a transceiver. Besides, as in an industrial WSN the deployment of the network can be planned, the LQE nodes, routers and sink nodes can be placed in locations with available power supply.

### 3.1. LQE node design and implementation

Fig. 2 shows a block diagram of the LQE node associated to one WSN node, and an image of the prototype developed to perform the experiments. This embedded system is composed by two micro-controllers, and two 2.4 GHz IEEE 802.15.4 transceivers. Each micro-controller is connected to one transceiver, using a Serial Peripheral Interface (SPI) bus, and to one serial port, to send data to a computer. The two micro-controllers are connected to each other using a bus of 10 bits, that can be used to exchange data between the LQE node and the WSN node in which it is associated (e.g. sink or CH node). The 10 bits bus is composed by one interrupt bit, and nine data bits. MRF24J40MA transceivers, and PIC18LF4620 micro-

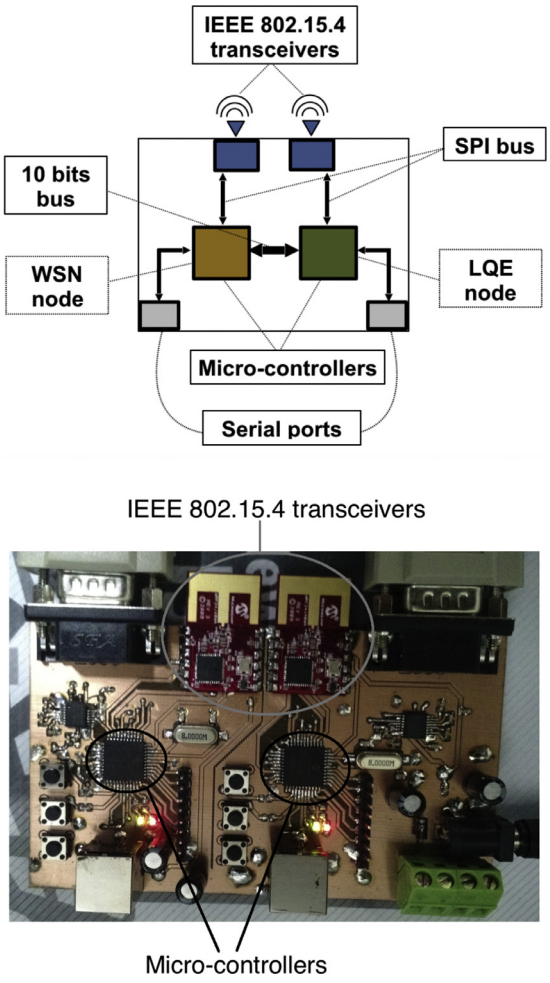


**Fig. 2.** Block diagram of the LQE node and the prototype used in the experiments.

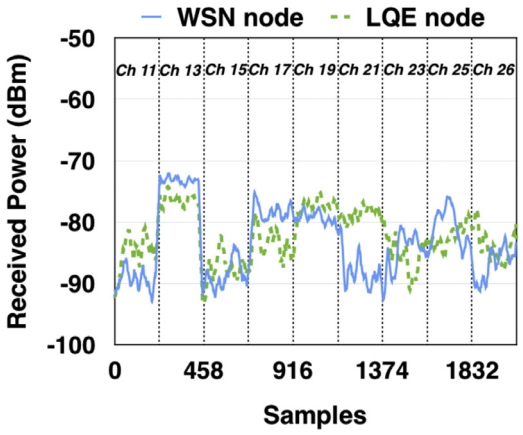


**Fig. 3.** Received power in the WSN node and in the LQE node.

controllers were used to build the prototype. The MRF24J40MA has a PCB antenna with a gain of 2.09 dBi, and a transmit power of 0 dBm.

An experiment was performed to verify the correlation between the values of RSSI obtained from each node, in nine different channels. Fig. 3 shows the received power in each node, calculated using the RSSI of the received packets. The values were filtered using a mean filter, with a window of 20 samples, to better analyze the shadowing in each channel. The nodes received packets in each channel during about 3 min, with a rate of one packet per second. As in this experiment the goal was to analyze the correlation between the signals received in both transceivers, the rate used is not related to a specific application. However, there are applications that use similar rates. For example, in the system described in [3], rates equal to 0.3 packets per second and 1.56 packets per second are considered.

The transmitter was positioned with a distance of about 23 m from the LQE node, and without line-of-sight. The nodes were configured remotely using another node, designed to communicate to each node the channel to be used in the next replication. This was done that way to avoid a change in position of the nodes involved in the experiment.

It is possible to notice that the multipath affects differently each channel. For example, the channels 11 and 13 presented a difference of about 15 dB in the mean value of received power. Although the values obtained from both nodes presented some correlation, the overall correlation was of about 47% (Pearson correlation). The antennas are separated with a distance of about 2 cm from each other. This correlation is compatible with the results observed in [23] for this distance. The most significant difference was observed when using Channel 21. During this replication, an exchange of staff occurred at the plant, which caused a high movement of people around the nodes. This may have generated a significant difference in the set of rays received in each antenna.

Due to this relatively low correlation, the proposed estimator uses values of RSSI obtained from the WSN node to perform the estimation. However, all processing is done in the LQE node. For each received packet, the WSN node that is associated to the LQE node transfers the RSSI value of the packet using the 10 bit bus that connects the two micro-controllers. Besides the RSSI value, one bit is also passed to the LQE node to indicate if the received packet is duplicate; that is, if it has the same identifier of the previous received packet. This is used to estimate the quality of the backward link. This procedure is performed using few instructions. In the prototype, a clock of 32 MHz (crystal of 8 MHz with 4X Phase Lock Loop) was used. In the device PIC18LF4620 each instruction cycle takes four clock cycles, and this procedure takes less than 4 µs (32 instructions cycles), which causes a small overhead on the WSN node. In the next section the proposed estimator is described and more details about its implementation in the prototype are provided.

## 4. The link quality estimator

This section describes experiments performed in real industrial environments. The data obtained from the experiments were used to develop the models that are used to implement the estimator. The proposed estimator is executed at the receiver side, and combines three metrics, the $P_f$, $C_a$, and $P_b$. The $P_f$ is based on the analysis of the RSSI of received packets, and captures the effects of fading and shadowing in the channel quality. It has high correlation with the PRR at the receiver (forward PRR). The $C_a$ is based on the analysis of RSSI values obtained in periods without packet reception, and captures the influence of interference sources in the channel quality. The $P_b$ is based on the number of duplicate packets received, and has high correlation with the PRR at the transmitter (backward PRR). Using the metrics it is possible to obtain a holistic characterization of the link.

Transceivers, fully compliant with the IEEE 802.15.4 standard, were used in the experiments, which implement the CSMA/CA mechanism in the MAC layer. However, the developed models are not dependent on the CSMA/CA mechanism, since it uses information from physical layer (RSSI), and information about duplicate packets, that is also independent from the MAC protocol. Thus, the models can be applied for transceivers that implement other MAC protocols, such as in the WirelessHART, and ISA100 standards.

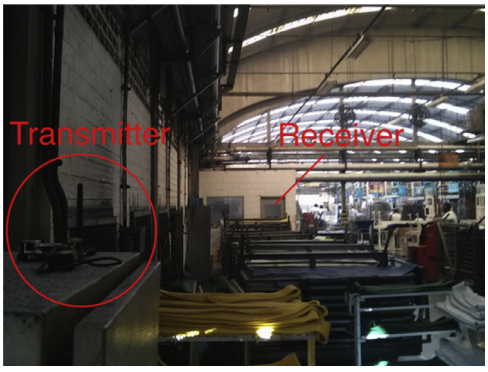


**Fig. 4.** Environment where the experiments were performed for the Scenario 1.


**Fig. 5.** Environment where the experiments were performed for the Scenario 2.

These standards use Time Division Multiple Access to reduce collisions and the energy consumption. In addition, they use frequency hopping and blacklisting, to mitigate the problems related to interference and fading. However, without an adequate management of the blacklist, the communication performance may be low for these standards [42].

### 4.1. Estimation of the forward link quality

Experiments in an actual industrial environment were performed to obtain plots of RSSI, LQI, and the PRR, for different channels and two different scenarios. Two nodes were used, one for the transmitter and one for the receiver. Five replications were performed for each scenario and for each channel considered. In each replication, the transmitter was configured to transmit 1000 broadcast packets (without ACK and retransmission) with a rate of 10 packets per second. Each packet had 70 bytes of payload, including a identifier. The receiver was configured to perform readings of RSSI, and LQI values, and the identifiers of each received packet. The information obtained at the receiver was transmitted via a serial port to a computer. Before each replication, the nodes were configured using a third node, to avoid a change in position of the transmitter and the receiver.

No specific application was considered for this experiment. However, there are applications that use similar transmission rates. For example, in the system described in [1] the packets carried 72 bytes of payload, and the sensor nodes transmit at a rate of 20 packets per second during the transmission periods. For the system described in [2], packets with 96 bytes of payload are transmitted at a rate of 4 packets per second.

The nodes used in this experiment are composed of a PIC18LF4620 micro-controller, and an IEEE 802.15.4 transceiver, the MRF24J40, with transmit power of 0 dBm, and an omnidirectional antenna, with a gain of 3 dBi.

In the first scenario, the nodes were placed at a distance of about 13 m, with line-of-sight. In this scenario, there were few metallic objects near the nodes. Fig. 4 shows the transmitter and the location where the receiver was placed in the first scenario. For this scenario, experiments for channels 11, 13, 15, 19, and 21 were performed. In the second scenario, the nodes were placed at a distance of about 30 m without line-of-sight. In this scenario there were several metallic objects near the nodes. Fig. 5 shows the transmitter in the second scenario. The receiver was placed in the same location of the first scenario. For this scenario, experiments for channels 11, 15, 19, and 21 were performed.

To analyze the channel characteristics, two metrics were obtained from the RSSI and LQI plots. The first metric, called $R_{avg}$ is the mean value of the normalized RSSI or LQI, and the second metric, called $d_{avg}$, represents the average variation of the signal in relation to the mean value. Before calculating $R_{avg}$, the RSSI and LQI plots were filtered using a median filter, to eliminate possible outliers. The $d_{avg}$ metric was obtained using Eq. (2).

$$d_{avg} = \frac{\sum_{V_i \in M_R} \left| 1 - \frac{V_i}{R_{avg}} \right|}{|M_R|}, \tag{2}$$

in which $M_R$ is the set of values of RSSI or LQI obtained in one replication, normalized.

As no interference source was present in the environment during this experiment, the differences in PRR, $R_{avg}$ and $d_{avg}$ in each replication are only due to the shadowing and fading. Thus, the model described in this section is capable of capturing the channel quality, regarding the effects caused by the multipath profile of the environment in the channel.

In Scenario 1, the PRR was high, since there was line-of-sight between the transmitter and the receiver, with a small distance between them. However, there was some difference in the values for each channel, and Channel 15 presented the best quality, with 99.8% of PRR, in average, while Channel 13 presented the worst quality with 96.8% of PRR, in average. In Scenario 2, the PRR was lower, since there was no line-of-sight between the transmitter and the receiver, and the distance was about 30 m. Besides, there were several metallic objects near the transmitter. In this scenario, Channel 15 also presented the best quality, with a PRR of about 84.2% in average. Channel 19 presented the worst quality, with 66.6% of PRR, in average.

Figs. 6 and 7 show the results when using RSSI, and LQI to compute the metrics, respectively. In all charts the PRR is marked on the Y axis. All values are presented in percentage. Fig. 6(a) shows the relation between the $R_{avg}$[RSSI] metric and the PRR considering the two scenarios together, and Fig. 6(b) shows the relation between the $d_{avg}$[RSSI] metric and the PRR. Fig. 7(a) shows the relation between the $R_{avg}$[LQI] metric and the PRR considering the two scenarios together, and Fig. 7(b) shows the relation between the $d_{avg}$[LQI] metric and the PRR.

In the charts shown in Figs. 6(a) and 7(a), the values regarding Scenario 2 are concentrated on the left, since the maximum value of $R_{avg}$[RSSI] for this scenario was 12.46%, and the maximum value of $R_{avg}$[LQI] was 42.6%. In the charts shown in Figs. 6(b) and 7(b), the values regarding Scenario 2 are concentrated on the right, with $d_{avg}$[RSSI] larger than 28%, and with a higher dispersion, and with $d_{avg}$[LQI] larger than 2.9%.

The metric $d_{avg}$[RSSI] presented a higher correlation with PRR in Scenario 1 and the metric $R_{avg}$[RSSI] had better correlation in Scenario 2. This can be explained due to the low amount of fixed metallic objects near the nodes in Scenario 1, which diminish the amount of time-invariant rays, and thus the small-scale variation dominates in Scenario 1. On the other hand, there were many fixed metallic objects near the transmitter in Scenario 2 causing

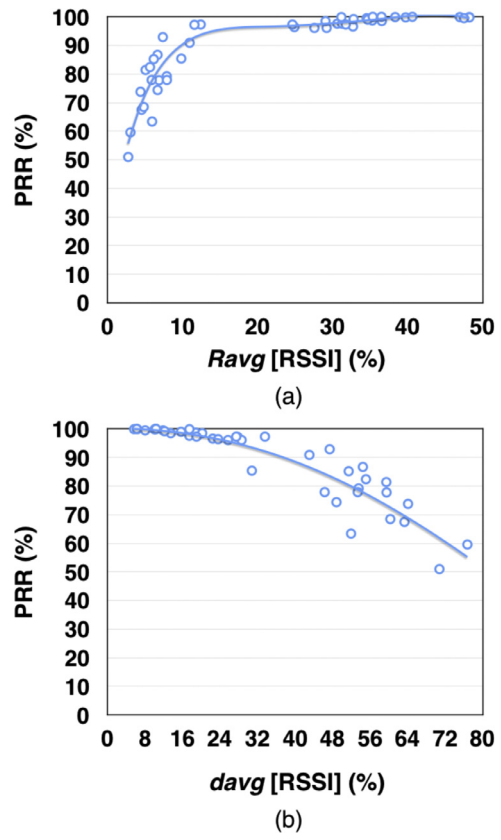


**Fig. 6.** (a) $R_{avg}$ versus PRR using RSSI. (b) $d_{avg}$ versus PRR using RSSI.

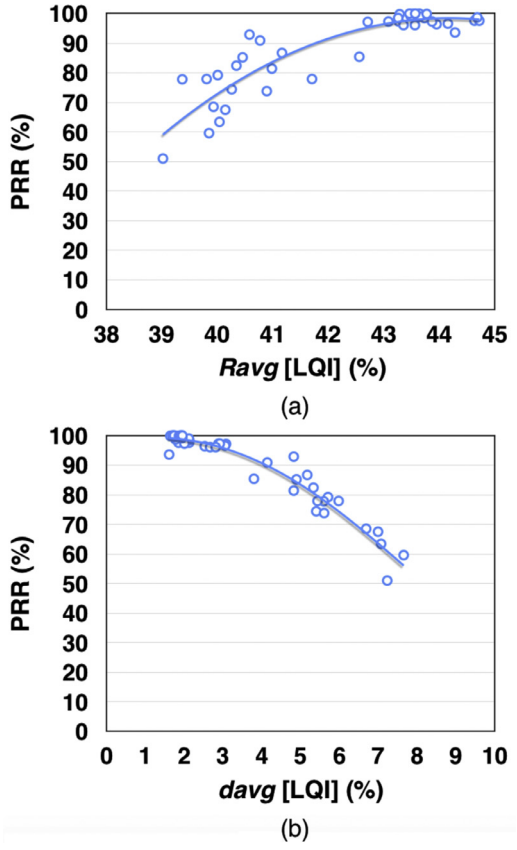


**Fig. 7.** (a) $R_{avg}$ versus PRR using LQI. (b) $d_{avg}$ versus PRR using LQI.

the presence of many time-invariant rays that influence the shadowing.

When using LQI, the $d_{avg}$[LQI] presented a higher correlation than $R_{avg}$[LQI]. As discussed in Section 2.2.1, the implementation of LQI is vendor-specific [27], which makes difficult to develop a general solution using this metric. For example, in [25,43] the LQI presented high variance in the experiments, using the CC2420 transceiver, from Texas Instruments, and in [44] the values of LQI varied very low using the MRF24J40 transceiver from Microchip, even in very different scenarios. In this paper, MRF24J40 transceivers were used. It is possible to see from Fig. 7 that the values of the metrics remained within a small range when using LQI, due to the low variation of this metric on MRF24J40 transceivers. When using RSSI it was possible to observe a higher difference between the values obtained for the two different scenarios. Because of those limitations of LQI, the RSSI was chosen in this paper to develop the model to estimate the forward link quality.

Based on the results, two approaches to estimate the forward link quality were implemented. The first one is based on two Artificial Neural Networks (ANN), using the metrics $d_{avg}$[RSSI] and $R_{avg}$[RSSI] as parameters, and the second one is based on a polynomial model, using only $R_{avg}$[RSSI] as parameter. In the rest of this paper $d_{avg}$[RSSI] will be referred simply as $d_{avg}$, and $R_{avg}$[RSSI] as $R_{avg}$.

In the first ANN, there are two neurons in the input layer, that receive as input the metrics $d_{avg}$, and $R_{avg}$, respectively, eight neurons in the hidden layer, and one neuron in the output layer, that generates the estimated forward link quality ($P_f$) as output. In the second ANN, there is only one neuron in the input layer, that receives the metric $R_{avg}$ as input. Tests were performed varying the number of hidden neurons from one to ten neurons, and the best result was obtained for eight neurons. This topology is simple and can be easily executed in a sensor node. As the values processed by the ANN are real, varying from 0 to 1, a sigmoid function was used as the activation function.

Half of the values obtained in the experiments were used to train the ANN, and the other half were used for validation. Values obtained from a third experiment (in open field, without metallic objects and with line-of-sight) were also used for validation. The desired error for the ANNs was set to 0.0001. The first ANN converged after 3560 epochs, with an error of 0.0001. The second ANN converged after 800,000 epochs, with an error of 0.000116.

Since the $R_{avg}$ metric captures an important characteristic for scenarios in which there are many time-invariant rays, such as in Scenario 2, for this type of scenario only this metric was used. For the Scenario 2 the use of the metric $d_{avg}$ causes a higher error in the estimation in comparison with the use of only the $R_{avg}$ metric. On the other hand, for the Scenario 1 the value of $d_{avg}$ is very important, which provides information about the small-scale fading. In this scenario, the effect of the shadowing did not cause a high difference in PRR.

Thus, for values of $R_{avg}$ higher than 0.1, the first ANN is used (with $d_{avg}$ and $R_{avg}$ as parameters), and for values of $R_{avg}$ less or equal to 0.1 the second ANN is used (with $R_{avg}$ as parameter). According to the results shown in Fig. 6, this threshold is a good approximation to distinguish the two types of scenarios considered.

The second approach uses a polynomial regression model, using only the $R_{avg}$ as input. The best fit to the curve was obtained with a polynomial of degree six, with a coefficient of determination ($R^2$) equal to 0.9464. With the polynomial model the $P_f$ can be obtained using

$$P_f = -3943.5R_{avg}^6 + 6506.6R_{avg}^5 - 4279R_{avg}^4 + 1430.9R_{avg}^3 - 256.47R_{avg}^2 + 23.77R_{avg} + 0.022. \quad (3)$$

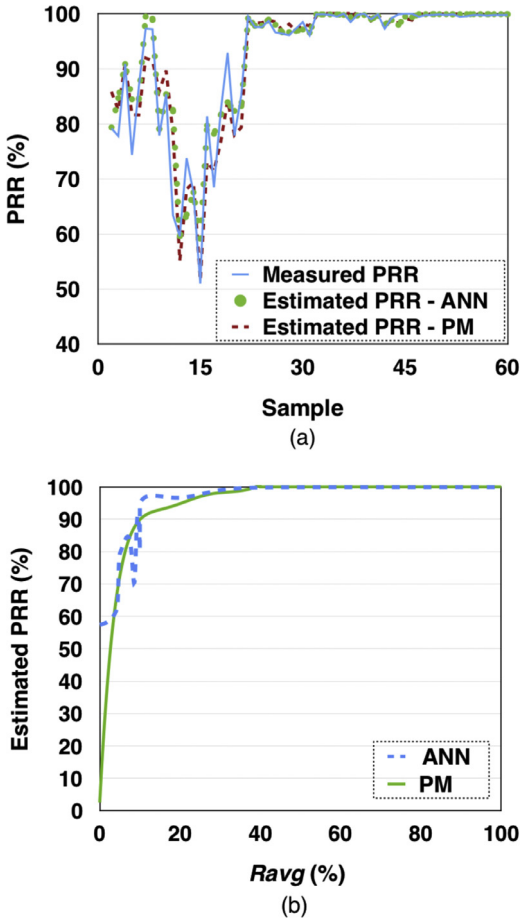


**Fig. 8.** (a) Validation of the values obtained from the ANN-based model and from the polynomial model. (b) Values provided by the models for all possible values of $R_{avg}$.

**Table 1**
Correlation between $P_f$ and PRR for each model.

| | ANN model | Polynomial model |
|---|---|---|
| Correlation | 82.5% | 88.1% |
| *p*-value | $4.97 \times 10^{-16}$ | $1.75 \times 10^{-20}$ |
| Mean absolute error | 1.74 | 2.23 |

Fig. 8(a) shows the measured PRR for all replications performed in the three scenarios (Scenarios 1 and 2 in the industry, and Scenario 3 in an open field) and the values estimated using the ANN-based model, and using the Polynomial Model (PM) according to Eq. (3).

Table 1 shows the Spearman correlation, the *p*-value, and the mean absolute error for each approach.

From the result, it is possible to observe that the models were able to estimate the PRR for all scenarios considered for validation, with good accuracy. However, since the data set used to train the ANN does not cover all ranges of values of PRR and $R_{avg}$, the ANN model did not generalize for values of PRR less than 50%. On the other hand, the polynomial model is capable to provide response for all range of values of $R_{avg}$ and PRR, as can be seen in Fig. 8(b). In addition, the polynomial model provided a higher correlation with the measured forward PRR, and is less computationally complex than the ANN model. Thus, it was used to implement the proposed estimator.

The noise floor can vary for different nodes in the network and over time [45], thus to obtain a better accuracy, it may be necessary to use the Signal-to-Noise Ratio (SNR) value instead of the RSSI directly. However, for the experiments performed for this paper, the noise floor remained below the sensitivity threshold of the transceiver for all channels during almost 100% of the time. For example, during the experiments described in Section 4.2, to identify interference problems, more than 97% of the RSSI values acquired on Channel 26 were equal to zero, and for the other channels the RSSI also remained most of the time equal to zero, except in the case of spikes due to external interference sources. Channel 26 is the only one of the IEEE 802.15.4 standard that is free of interference from IEEE 802.11 networks [45].

In other environments, it may be necessary to subtract the value of RSSI related to the noise floor from the RSSI values of the packets before computing the metrics, in order to obtain a better accuracy. By using the LQE node, RSSI values are acquired continuously to identify interference problems, so it is also possible to measure the noise floor in real time using the samples of RSSI acquired at the LQE node, without causing overhead on the WSN node.

The RSSI values associated to the packets are measured over the first eight symbols of the packet. Thus, the measured RSSI is independent of the packet size. For larger packets, the probability of reception can be smaller in some cases. However, the bit-error distribution is uniform for corrupted packets, due to fading problems, as observed in the experiments described in [15]. On the other hand, for packets corrupted by Wi-Fi interference, the further a bit is from the beginning of the packet, the higher the probability that it will be corrupted [15].

Thus, only in scenarios with external interference the packet size could cause a significant impact on the estimation. However, as $P_f$ is only used to estimate the channel quality regarding fading and shadowing problems, the packet size may not influence significantly the estimation. Besides, packets with 70 bytes of payload were considered in the experiments, which is large enough for many applications. In scenarios with external interference, using only $P_f$ may overestimate the link quality, but in the approach proposed in this paper, the influence of interference is also measured, through other metric, called $C_a$ (described in Section 4.2). Thus, it is possible to accurately estimate the link quality both in scenarios with and without interference.

The model described in this section can capture the channel quality at the receiver side, regarding the effects caused by the multipath profile of the environment. As discussed in Section 2.1, abrupt changes can occur in the characteristics of the channels over time. Thus, a channel can present good quality for several minutes or hours, and begins to present low quality, due to some significant change in the multipath profile of the environment. The described model is capable to identify these changes in the channel quality.

The use of a dedicated node is important in this approach, since many values of RSSI need to be acquired to compute the metrics with accuracy. Besides, it is necessary to monitor multiple connections simultaneously. Using a dedicated node the execution of the estimator can be done without impairing the WSN operation.

#### 4.1.1. Evaluation for different packet transmission rates

The results shown in Section 4.1 have considered the values of RSSI obtained from all received packets during a period of 100 s. During this time interval, 1000 packets were transmitted with a rate of 10 packets/s. However, in some applications, the Packet Transmission Rate (PTR) can be less than 10 packets/s. To investigate the accuracy of the estimator for other values of PTR, an evaluation was made considering a PTR equal to 10, 5, 1, 0.5, and 0.2 packets/s, and considering a shorter time interval of acquisition. In the analyzes made in this section the measured PRR was obtained by calculating a new value for every 200 received packets. To obtain the value of $P_f$ considering values of PTR lower than 10 packets/s, values of RSSI were discarded from the original plot

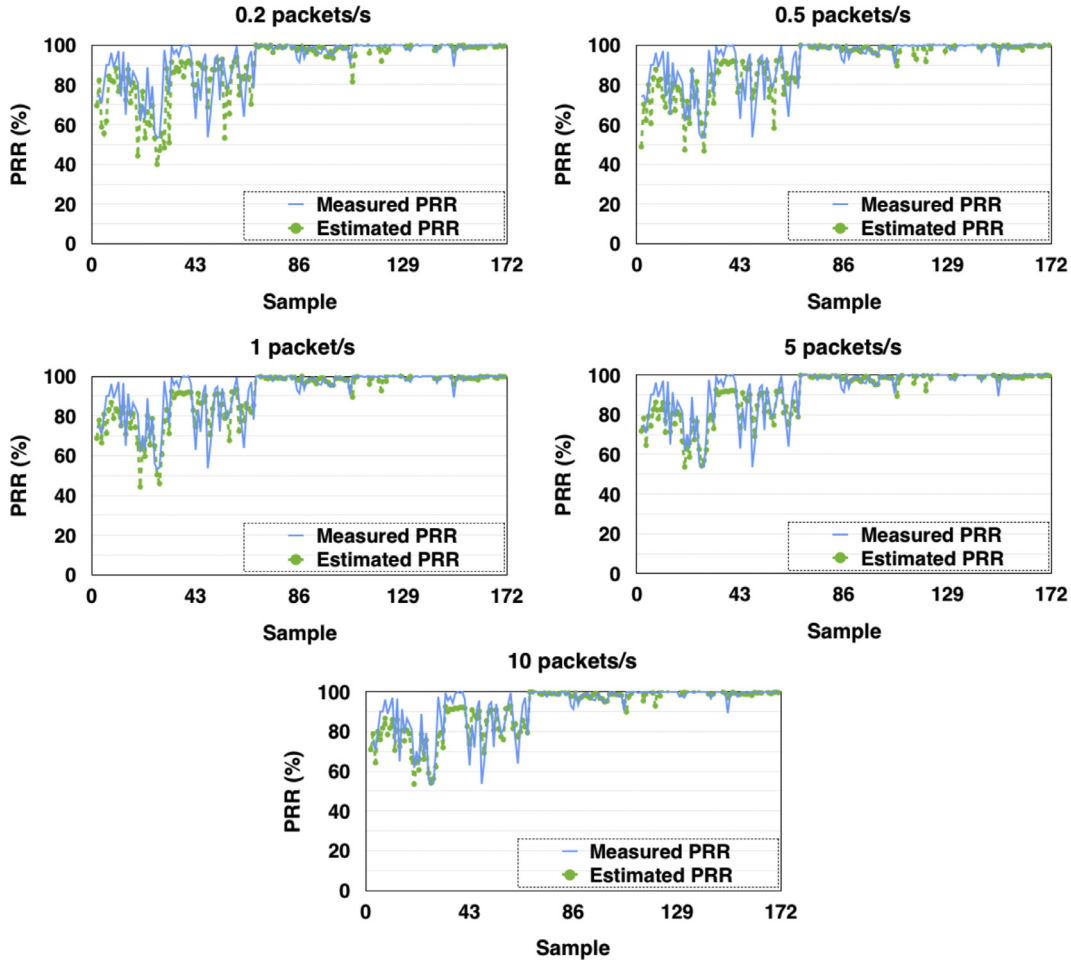


**Fig. 9.** Values obtained from the polynomial model for different packet transmission rates.

**Table 2**
Correlation between $P_f$ and PRR for each PTR, using the polynomial model.

| | Correlation | *p*-value |
|---|---|---|
| 0.2 packets/s | 80.4% | $5.55 \times 10^{-40}$ |
| 0.5 packets/s | 82.4% | $1.5 \times 10^{-43}$ |
| 1 packet/s | 84.0% | $9.93 \times 10^{-47}$ |
| 5 packets/s | 84.7% | $2.37 \times 10^{-48}$ |
| 10 packets/s | 84.7% | $3.45 \times 10^{-48}$ |

**Table 3**
Correlation between $P_f$ and PRR for each PTR, using the polynomial model, considering only the Scenario 2.

| | Correlation | *p*-value |
|---|---|---|
| 0.2 packets/s | 56.6% | $6.01 \times 10^{-7}$ |
| 0.5 packets/s | 70.2% | $3.60 \times 10^{-11}$ |
| 1 packet/s | 77.4% | $1.5 \times 10^{-14}$ |
| 5 packets/s | 81.7% | $3.39 \times 10^{-17}$ |
| 10 packets/s | 82.5% | $9.99 \times 10^{-18}$ |

uniformly. Thus, for each estimation a set of 200, 100, 20, 10, and 4 values of RSSI were used, for PTRs equal to 10, 5, 1, 0.5, and 0.2 packets/s, respectively.

Fig. 9 shows the curves of the measured and estimated PRR for each PTR considered. By a visual analysis of Fig. 9 it is possible to observe an increase in the difference between the measured and the estimated PRR for the lowest values of PTR (0.2 and 0.5 packets/s), as expected. However, the differences are less evident when considering values of PTR equal to 1 packet/s, 5 packets/s and 10 packets/s.

Table 2 shows the Spearman correlation, and the *p*-value, for each PTR, considering the two scenarios on the industrial environment. In this case, for all values of PTR the correlation was high, and the correlation for 5 packets/s and 10 packets/s was the same. Table 3 shows the values considering only the Scenario 2, in which a higher variation in PRR is observed. In this case, the correlation for 0.2 packets/s was low, and higher differences were observed for the different values of PTR.

Even with lower values of PTR it is possible to estimate the forward link quality. For values of PTR higher than 0.5 packets/s the correlation between measured and estimated PRR was high for the acquisition interval used, even when considering only Scenario 2. However, if the PTR is very low, the acquisition interval needs to be increased, since it is not possible to proper estimate the channel quality using only a few samples of RSSI, as discussed in Section 2.2.1. For example, considering a PTR equals 0.2, it is necessary to acquire values during a few minutes to obtain a good accuracy. However, for many industrial WSN, such as the ones described in [1–3], which use PTR larger than 1 packet/s, shorter acquisition intervals can be used.

In less dynamic environments, such as in the experiments described in [17], acquiring values for some minutes is acceptable, since the channel remains stationary for a longer period of time

(7 h in their experiment), in which the mean reception power remains constant. Other alternative is to transmit some empty packets during times of no operation of the sensor nodes, which allows a better estimation, but consumes more resources of the sensor nodes. However, the analysis of these trade-offs is application-specific.

It is worthy to notice that the metric $P_f$ is used only to estimate the channel quality regarding fading and shadowing problems. In the approach proposed in this paper, the influence of interference is assessed through other metric (explained in Section 4.2). Thus, even for WSN that use a low PTR, interference problems can be identified promptly using the LQE node and the metric described in Section 4.2. In Section 5, a PTR equal to 1 packet/s was used to validate the proposed LQE and the LQE node, using the model described in this section, and the models described in Sections 4.2 and 4.3.

### 4.2. Estimation of the interference influence

Some devices can cause interference in the 2.4 GHz band, such as microwave ovens, but these devices are not usually present in the industry [46]. Most industrial devices, such as electrical motors and frequency inverters, present interference only in the range of a few megahertz, therefore, no interference is experienced by radios that use the band of 2.4 GHz [19]. On the other hand, Wi-Fi networks can cause highly destructive interference in WSNs [1].

Although Wi-Fi networks can cause high interference on WSNs, it is possible to obtain a good quality of service, depending on the application requirements and the traffic of the Wi-Fi networks. For example, in the experiments described in [47] the channel remained free during about 60% of the time in periods with active Wi-Fi traffic. Besides, the Wi-Fi traffic is bursty, and leaves white spaces that can be used by the WSN nodes to communicate.

The model described in Section 4.1 is capable to identify multipath problems, but does not captures the effect of interference. As only RSSI values of received packets are used to calculate $P_f$, this metric can present a high value, even with a high number of lost packets due to collisions. Thus, it is necessary to capture the interference effects to properly estimate the quality of the link.

In the experiments described in Section 4.1 no interference source was present. Other experiments in the same industry were performed in an environment with external interference caused by Wi-Fi networks, operating in the channels 1, 6 and 11. A scan was made using a laptop, and seven Wi-Fi networks in Channel 1, four in Channel 6, and five in Channel 11 were identified. At the time of the scanning, the average signal's power of the Wi-Fi networks was −64.8 dBm for Channel 1, −75.3 dBm for Channel 6, and −66.2 dBm for Channel 11.

Fig. 10(a) shows the values of RSSI (from 0 to 255) obtained from channels 13, 17, and 23 during 5 s with a rate of 200 samples/s, with only the Wi-Fi networks active. The Channel 13 overlaps with the Channel 1 of Wi-Fi, the Channel 17 overlaps with the Channel 6 of Wi-Fi, and the Channel 23 overlaps with the Channel 11 of Wi-Fi. The interference was more severe for Channel 13. This is compatible with the amount of Wi-Fi networks operating in each channel. The values of RSSI obtained from Channel 17 are lower, due to the lower signal power of the Wi-Fi networks on Channel 6. The threshold line in the chart corresponds to a RSSI equal to 10.

To estimate the impact of interference it was used the channel availability ($C_a$) as the metric, similar to the metric used in [28]. To calculate $C_a$ the LQE node acquires values of RSSI using its transceiver, during the periods without packet reception. Using the LQE node it is possible to acquire many values of RSSI to analyze the interference impact without impose overhead on the WSN

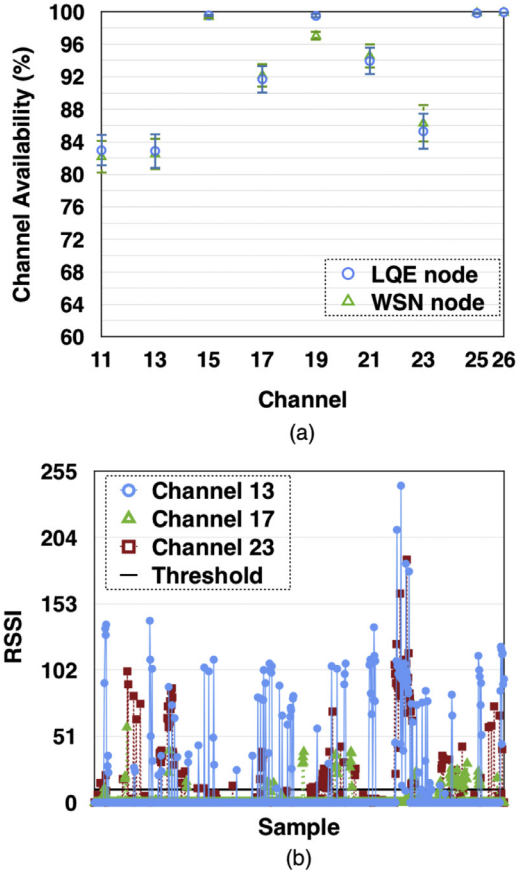


**Fig. 10.** (a)Interference in channels 13, 17, and 23. (b) Channel availability in nine different channels.

node associated to it. The channel availability is calculated using

$$C_a = 1 - \frac{\sum_{i=0}^{i<n} b_i}{n}, \tag{4}$$

in which $n$ is the number of samples used to calculate $C_a$, and $b_i$ is equal to 0 or 1 depending on the value of a threshold ($\tau$). The values of $b_i$ is calculated using

$$b_i = \begin{cases} 0, & \text{if } R_i < \tau; \\ 1, & \text{if } R_i \geq \tau; \end{cases}, \tag{5}$$

in which $R_i$ is the value of RSSI acquired in the $i$th sample.

As discussed in Section 3.1, the correlation between the signals received in the transceiver of the LQE node and in the transceiver of the WSN node can be relatively small in some cases. Thus, it was studied if it is possible to accurately calculate $C_a$ using values of RSSI acquired at the LQE node.

Fig. 10(b) shows the mean values of $C_a$, in percentage, for nine different channels, and calculated using values of RSSI acquired from the two nodes simultaneously. To calculate the values of $C_a$ it was used a value of $n = 200$ (an interval of 1 s). The nodes acquired RSSI values in each channel during about 1 min. A confidence level of 95% was used. A threshold $\tau = 10$ was used, which is enough to differentiate between noise floor, and interference. Analyzing the values obtained for Channel 26, which does not overlap with any channel of Wi-Fi, the RSSI presented an average value equal to 0.021, and a standard deviation equal to 1.074.

Only the values for Channel 19 presented a significant difference, in which the mean value for the LQE node was equal to 0.99, and the mean value for the WSN node was 0.97. Since a threshold value is used, the differences between individual values of RSSI acquired from each transceiver cause a less impact for this metric.

Thus, it is viable to calculate the $C_a$ using the RSSI acquired from the LQE node.

Even with the presence of many Wi-Fi networks on channels 1, 6, and 11, some channels of the WSN remained free of interference. From Fig. 10(b) is possible to see that the channels 11 and 13 of the WSN, which overlap with Channel 1 of Wi-Fi, have the lowest availability among all channels evaluated.

### 4.3. Estimation of the backward link quality

The $P_f$, and $C_a$ metrics are capable to identify the channel quality at the receiver, regarding multipath problems, and interference. However, to characterize the overall quality of the link it is necessary considers the backward link quality, since the links are usually asymmetric [25]. Many applications use packet acknowledgment and retransmission, and control packets may also be transmitted to the end nodes.

The estimators that considers link asymmetry usually use probe broadcast packets, such as in the ETX [10], Four-Bit [11], F-LQE [12], and Opt-FLQE [13]. Some estimators, such as Four-Bit and Opt-FLQE, also compute an estimate of the RNP at the transmitter, which implicitly captures the quality of the both directions of the link. These estimators cause overhead on the network due to the probe packets, and perform processing on the transmitter to calculate the backward PRR or the RNP. Usually the transmitters are the end nodes of the WSN, which have more severe resource constraints in comparison with the sink nodes and CH nodes. Thus, the estimator proposed in this paper uses only information obtained at the receiver (ex: sink node, or CH node associated to the LQE node), and performs all the processing in the LQE node.

For each received packet, the WSN node that is associated to the LQE node transfers the RSSI value of the packet, and one bit to indicate if the received packet is duplicate, using the 10 bit bus that connects the two micro-controllers. A packet duplication occurs when the packet is received successfully, but the ACK packet does not is received correctly at the transmitter. Thus, the correlation between the number of duplicate packets and the backward PRR was studied, and a model was developed to estimate the backward link quality using this information.

Experiments were performed to obtain the total number of received packets, and the number of duplicate packets at the receiver for three different channels (11, 15, and 25). In each replication the transmitter was configured to transmit 1800 unicast packets with a rate of 1 packet per second (30 min). Each packet had 70 bytes of payload, including a identifier. The maximum number of retransmission attempts was equal to two.

To obtain the real backward PRR, the transmitter saved in its memory the total number of transmitted packets (including the retransmissions), and the total number of ACKs received in intervals of 10 s, during all the replication. At the end of the replication, the data saved on the transmitter was downloaded using a serial port. The nodes of the experiment used an MRF24J40MA transceiver, with a transmission power of 0 dBm, and a PCB antenna with a gain of 2.09 dBi. The location where the transmitter was positioned is shown in Fig. 13 on top (in Section 5).

Considering a window of $n$ received packets for the estimation, the average number of retransmissions per packet ($N_r$) is calculated using

$$N_r = \frac{N_d}{n - N_d}, \tag{6}$$

in which $N_d$ is the number of duplicate packets inside the set of $n$ packets.

Fig. 11(a) shows the relation between the $N_r$, and the measured backward PRR. As for this experiment the maximum number of retransmission attempts is two, it is the maximum value of $N_r$. It was used $n = 10$ in this experiment.

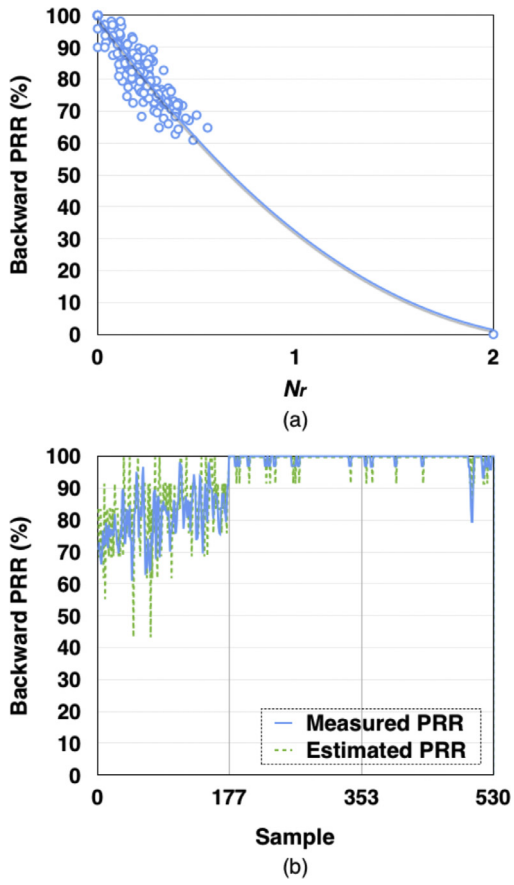


**Fig. 11.** (a) $N_r$ versus backward PRR. (b) Validation of the values obtained from the model.

Based on these measurements, a polynomial model was developed to calculate the estimated backward link quality ($P_b$) using the $N_r$ values. The best fit to the curve was obtained with a polynomial of degree two, with a coefficient of determination ($R^2$) equal to 0.9387. With the polynomial model the $P_b$ can be obtained using

$$P_b = 0.1785N_r^2 - 0.8485N_r + 0.997. \tag{7}$$

Fig. 11(b) shows the measured backward PRR, for all three replications, and the values estimated using Eq. (7). The Spearmans correlation between $P_b$ and the measured backward PRR was 88%, and the mean absolute error was 3.06. In the correlation analysis the $p$-value was $4.93 \times 10^{-174}$.

The backward PRR was worst in Channel 11 probably due to interference problems. The channels 15 and 26 were free of interference, as can be seen in Fig. 10(b). Analyzing the duplicate packets, the backward link quality can be estimated regardless the cause of failure in the reception of the ACKs.

## 5. Validation

To validate the proposed estimator, a set of experiments were performed to verify if the estimator is capable to accurately identify the link quality, and react fast to persistent changes in the link quality.

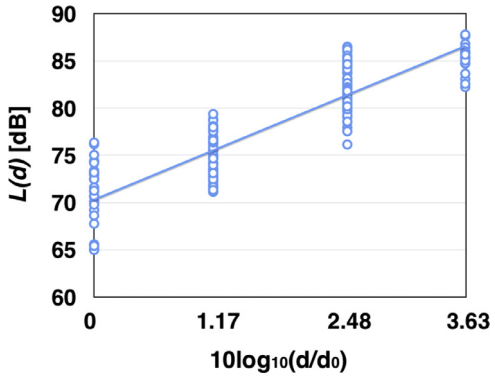


**Fig. 12.** Relation between the path loss and the distance between transmitter and receiver.

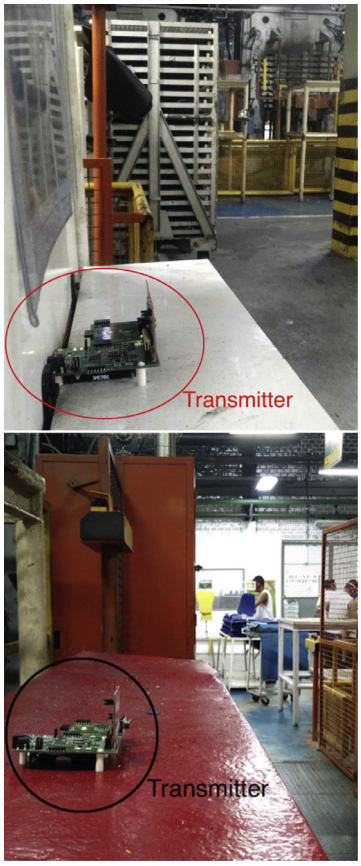


**Fig. 13.** Transmitters at the industrial plant.

### 5.1. Characterization of the industrial environment

The environment in which the experiments were performed, both to derive the models and to validate the proposed approach, has characteristics similar to other industrial environments considered in papers that performed experimental studies to characterize the wireless channel, such as [4] and [48].

With the values of RSSI obtained in the experiments described in Section 4.1, and in the experiments described in this section, it was possible to derive the parameters for the log-normal shadowing model, considering the values obtained for four different distances (13 m, 17 m, 23 m, and 30 m), and several different channels. Fig. 12 shows the relation between the path loss and the distance between transmitter and receiver. In the $X$ axis it was considered the value of $10log_{10}(d/d_0)$, in which $d$ is the distance between transmitter and receiver, and $d_0$ is the reference distance. To obtain the parameters of the model, the values obtained in Scenario 1 (see Section 4.1) were used as reference. Thus, $d_0 = 13$ m, and the path loss on the reference distance ($L(d_0)$) is equal to the mean reception power, considering all replications made for Scenario 1.

**Table 4**
Parameters for the log-normal shadowing model of the industrial environment where the experiments were performed.

| Path loss exponent ($n$) | Shadowing deviation ($\sigma$) | $d_0$ | $L(d_0)$ |
|---|---|---|---|
| 4.47 | 5.49 dB | 13 m | 70.3 dB |

Table 4 shows the values of the parameters obtained for the log-normal shadowing model. Even considering only a few samples of distance to derive the parameters, the obtained values are similar to the ones found in [4] for an industrial environment, and for the 2.4 GHz band. In [4] a more detailed characterization, in terms of path loss and fading in an industrial environment, can be found. In [48] the parameters for the log-normal shadowing model were found for different environments in the context of smart-grid applications, including industrial environments.

### 5.2. Validation of the estimator

The metrics $P_f$, $C_a$, and $P_b$ can be analyzed separately, or be combined to calculate the overall link quality ($L_q$), according to

$$L_q = P_f \times C_a \times P_b. \quad (8)$$

The proposed estimator, and the Opt-FLQE estimator were implemented to be executed in the prototype shown in Fig. 2. Two transmitters were configured to transmit unicast packets (with ACK and retransmission) with a rate of 1 packet per second, and broadcast probe packets with a rate of 0.2 packets per second. The LQE node also sends broadcast packets with the same rate. The broadcast probe packets were used to compute the Opt-FLQE estimator, since the LQE proposed in this paper does not use probe packets. The first transmitter was placed with 23 m of distance from the sink node (Fig. 13 on top), and the second transmitter and the sink node were placed 17 m apart (Fig. 13 on the bottom), without line-of-sight.

For the experiments described in this section, a window $n = 20$ data packets was used to compute $P_f$ and $P_b$, which is an interval of 20 s, in the best case, for this experiment. To calculate $C_a$ a variable number of samples was used, depending on the number of acquisitions between two packet receptions. The LQE node was configured to acquire RSSI with a rate of 200 samples/s, in periods without packet reception. A EWMA filter was used to smooth the values of $P_f$, $P_b$, and $L_q$, and make them more stable, and resistant to small and rapid variations on channel quality. The value $\alpha = 0.6$ was used for the EWMA filter. In [13] $\alpha = 0.9$ was used for the EWMA filter to calculate the final value of Opt-FLQE, but for this paper $\alpha = 0.6$ was used, to obtain more reactivity. The values used in Opt-FLQE were calculated using a window of five broadcast probe packets, which is an interval of 25 s, in the best case, for this experiment.

In the first experiment, Channel 20 was used during 30 min. In the second experiment, Channel 16 was used during 60 min. As in the experiments described in Section 4.3, the transmitters saved in memory the total number of transmitted packets, and the total number of ACKs received for each 10 s interval, during all the replication. The receiver was configured to transmit the identifier of all received packets to a computer using a serial port. With the data obtained from the transmitters, and from the receiver, it is possible to calculate the real PRR in both directions for each link after the experiments, to be used as a reference value.

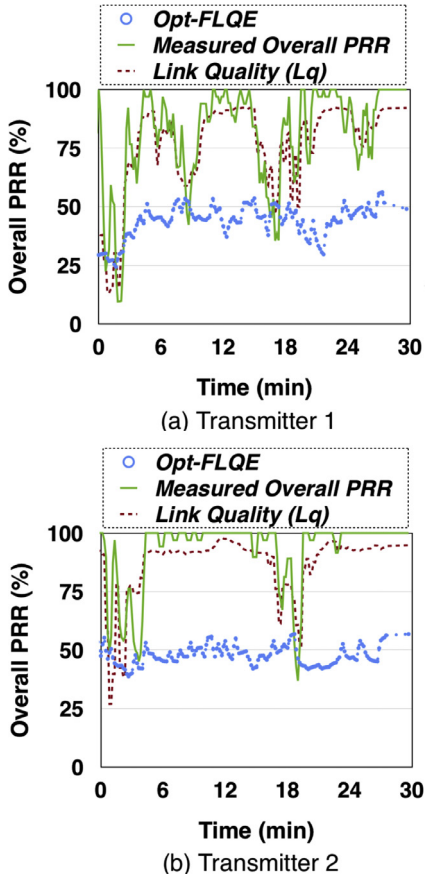


**Fig. 14.** Results for Channel 20, during 30 min.

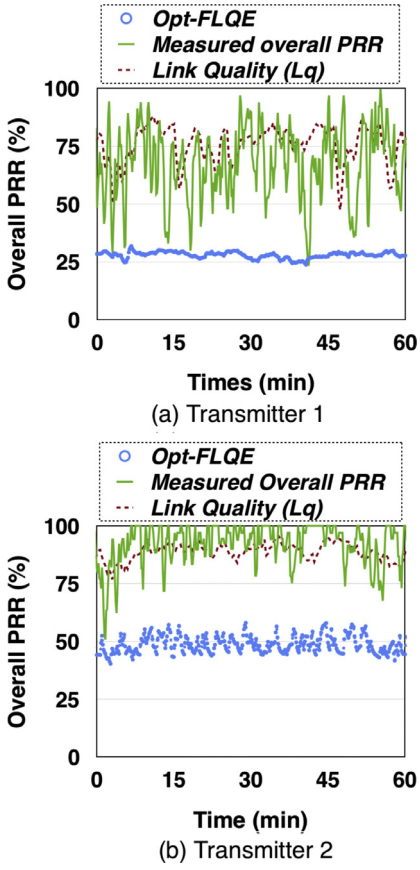


**Fig. 15.** Results for Channel 16, during 60 min.

Since two transmitters were used, one bit out of the 10 bits bus was used to transmit to the LQE node a identifier of the transmitter. Thus, only seven bits were used to transmit the RSSI values to the LQE node. Since for this scenario the values of RSSI are always less than 127, the use of seven bits is possible. To monitor the quality of a higher number of links more bits are needed to pass the RSSI values, the identifier of the transmitter, and the bit indicating a duplicate packet through the bus. This can be done with a larger bus or using two write operations on the bus. Since the time spent to transmit data using the bus is very small (less than 4 µs), this approach is viable. For future works, a new prototype with a 18 bits bus will be developed (one bit for interruption, and 17 bits for data).

As a reference to the estimated values, it was used the measured overall PRR of the link, that is, the multiplication of the PRR in both directions, that were calculated off-line, using the data saved on the transmitters, and with the trace generated by the receiver. Fig. 14 shows the measured overall PRR, and the values provided by the proposed estimator ($L_q$), and by the Opt-FLQE estimator for the replication with the Channel 20. Fig. 15 shows the results for the experiment using Channel 16. The link of Transmitter 1 presented a lower quality in both cases, since it is positioned at a more distant location from the receiver than Transmitter 2.

The values of Opt-FLQE varied around 50 for both links when using Channel 20 (Fig. 14), but for the Transmitter 1 the variation was higher, due to the higher variation of link quality for Transmitter 1. When using Channel 16, the value of Opt-FLQE varied around 25 for the link with the Transmitter 1, and around 50 for the link with Transmitter 2.

The values provided by the Opt-FLQE estimator, that are shown in Figs. 14 and 15, are compatible with the results described in [13], for the experiments with moderate links. The Opt-FLQE is very stable, but in some cases presents low reactivity to more persistent variations in link quality, as can be observed for the results from Fig. 14. For this scenario, the change in the channel quality that occurred at minute 15 only was noticed by the Opt-FLQE after about 3 min, while the $L_q$ reacted promptly.

**Table 5**
Correlation between the estimators and the measured PRR.

| | Opt-FLQE | Proposed estimator ($L_q$) |
|---|---|---|
| Correlation | 59.4% | 72.5% |
| $p$-value | $8.67 \times 10^{-102}$ | $8.99 \times 10^{-173}$ |

The proposed estimator ($L_q$) presented good accuracy, and reactivity, but it is less stable than the Opt-FLQE. However, it is capable to quickly identify abrupt and persistent changes in the link quality. The stability can be improved using a higher factor for the EWMA filter. The Opt-FLQE values are not a direct estimate of the overall PRR, which explains the high absolute difference between the overall PRR and the Opt-FLQE. However, these two metrics need to present a high correlation, since both are related to the overall link quality.

To compare the accuracy between the Opt-FLQE and the proposed estimator, the Spearman's correlation was calculated using as reference the measured overall PRR, and the data obtained from the two scenarios and for both transmitters. Table 5 shows the correlation and the $p$-value for each estimator. Both estimators have a relatively high Spearman's correlation, but the correlation for the proposed estimator is significantly higher than the correlation for the Opt-FLQE. The Opt-FLQE uses linear functions to compute the fuzzy variables, which is very simplistic. The proposed estimator

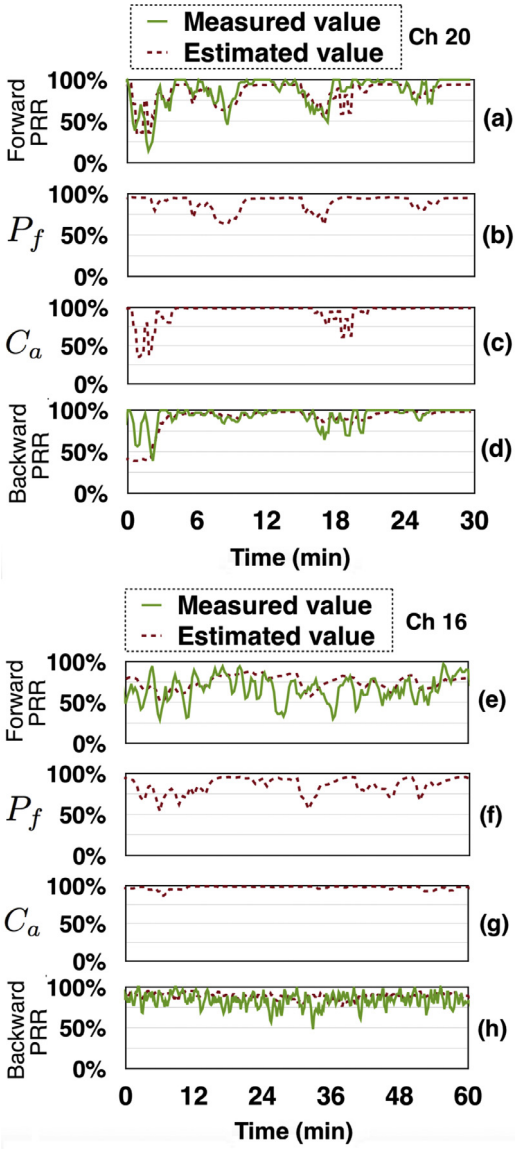


**Fig. 16.** Analysis of the metrics individually.

uses more elaborated models in the estimation, based in data obtained from experiments in real industrial environments.

Fig. 16 shows the analysis of the metrics individually, considering the link with the Transmitter 1, in channels 16 and 20. It is possible to notice that Channel 20 was more affected by interference sources, as can be seen in Fig. 16(c) and (g), which caused a high influence on the link quality in some time intervals. For example, for Channel 20, during the first 3 min, and around the minute 18 the $C_a$ was low, which caused a drop in quality for both links (Transmitter 1 and Transmitter 2), as can be seen in Fig. 14. Other variations in link quality, for Channel 20, was due to the variations on the channel quality, as can be seen in Fig. 16(b), that shows the values of $P_f$ during all replication.

In Channel 16 all the variation in the link quality was due to the channel quality, as can be seen in Fig. 16(f). Fig. 16(d) and (h) shows the backward link quality, both measured and estimated. For Channel 20 the backward link quality was also affected by the interference sources, which explains the similarities with the chart from Fig. 16(c). In general, the backward link quality was better for both channels, which shows the asymmetry of the wireless channel.

Different from other estimators, such as ETX, Four-Bit, F-LQE, and Opt-FLQE, the proposed estimator allows identify the main causes of a low link quality (channel quality, interference influence, or asymmetry) through the analysis of the metrics individually. It can help the protocols to make the better decision for each case. For example, when the link is affected by interference sources, as in the case illustrated in Fig. 16(c), change the route may not be very useful, mainly if the interference source also affects the transmitter, as in the case illustrated in Fig. 16(d).

In addition, a dynamic channel allocation mechanism needs to pick a channel with a certain spacing in frequency in this case, since most interference sources affects adjacent channels. When the low link quality is only due to a low channel quality, as in the case illustrated in Fig. 16(f), or due to asymmetry, change route or channel can help to improve the link quality. Those aspects will be the subject of a future work.

The execution time of the algorithms, to calculate $P_f$, $C_a$, and $P_b$, was approximately 40 ms (using a non-optimized, and free C compiler). Using the memory available in the low-cost 8-bit microcontroller PIC18LF4620 it is possible to monitor up to 60 links simultaneously. With an optimized C compiler (the Pro version) the execution time could be lower. To monitor 60 links simultaneously, the estimator would take 2.4 s to perform the calculations for all links, which allows the real-time monitoring of link quality using the LQE node, even in scenarios with many transmitters, since the wireless channel usually remains stationary for a period much longer than the time needed to estimate the link quality, as can be seen in [17,18]. Besides, the proposed estimator reacts quickly to abrupt and persistent changes in link quality, as demonstrated in this section.

The proposed estimator does not overload the nodes, or the network, since all processing is performed at the receiver side, using the LQE nodes, and the metrics are calculated using information extracted from received data packets. In the experiments described in this section, the Opt-FLQE increased the network traffic in 20%, due to the probe packets, and resources were spent at the end node, to calculate the values of PRR and SRNP, and to send and receive probe packets, which can cause a significant increase in the energy consumption, and can impair the execution of the main application. Even with this high increase in the network traffic, the Opt-FLQE presented low reactivity.

The values obtained from a window of 20 packets were used to compute the metrics. Thus, the time to acquire all samples can be of some minutes if the link quality becomes very poor. To mitigate this problem, a sliding window could be used to allow the computation of new values more often.

## 6. Conclusions and future work

This paper proposed the use of dedicated nodes (LQE nodes) to monitor the link quality in industrial WSN. The LQE nodes are associated to a receiver (e.g. sink node), and uses the RSSI, and information obtained from received data packets to identify interference and multipath problems that affect the link quality in both directions. This approach is viable for an industrial WSN, because its deployment can be planned.

In environments with high RMS delay spread, such as industrial plants, the channels are weakly correlated in frequency, and switching the channel can improve the quality of service of the network. The proposed estimator, and the LQE node, can be used to implement dynamic channel allocation mechanisms, and also other types of protocols, such as adaptive routing protocols, that considers the link quality, for industrial WSN.

A set of experiments was performed in a real industrial environment to investigate how the RSSI plots can be used to implement the LQE node. Models were developed to identify multipath,

and interference problems, using information obtained from the RSSI plots, which is not possible with the analysis of individual, or averaged values, of small samples of RSSI. The backward link quality is estimated using the information about duplicate packets on the receiver. Thus, different from other LQEs already proposed in literature, the LQE proposed in this paper does not generate extra traffic through the use of probe packets or redundancy in the packets, neither performs processing on the transmitter, which is usually the end node of the WSN.

The proposed LQE was validated through experiments performed in an industrial environment, and was compared to a state-of-the-art LQE, the Opt-FLQE. The proposed LQE showed a higher correlation with the measured overall PRR of the monitored links, and a higher responsiveness to abrupt changes in the link quality. The proposed solution can be applied for different WSN implementations, considering different MAC protocols (e.g. CSMA/CA or TDMA), and adaptive mechanisms (e.g. dynamic channel allocation or adaptive routing).

As an example, the DSME mode of the IEEE 802.15.4e standard defines a channel adaptation mechanism, in which a channel switch only occurs when the channel in use in a given time-slot starts to present low quality. Therefore, a procedure is necessary to evaluate the quality of the links continuously, in order to use the channel adaptation mechanism properly. However, the implementation of this procedure is not defined by the standard [40]. The solution proposed in this paper could be used to implement the channel adaptation mechanism of the DSME mode.

The development of dynamic multi-channel protocols, using the LQE node and the link quality estimator described in this paper, is proposed as future work. In addition, improved models for simulation will be developed to allow the simulation of multi-channel protocols in industrial environments. Finally, experiments with a large number of nodes will be performed, both using simulation, and experiments in real industrial environments.

## Acknowledgment

The authors would like to thank the support of the Institute for Advanced Studies in Communications (Iecom), the Brazilian Council for Research and Development (CNPq), the Coordination for the Improvement of Higher Education Personnel (CAPES), and Copele.

## References

[1] A. Lima-Filho, R. Gomes, M. Adissi, T. Borges da Silva, F. Belo, M. Spohn, Embedded system integrated into a wireless sensor network for online dynamic torque and efficiency monitoring in induction motors, IEEE/ASME Trans. Mechatron. 17 (3) (2012) 404–414, doi:10.1109/TMECH.2012.2187354.

[2] E. Sisinni, A. Depari, A. Flammini, Design and implementation of a wireless sensor network for temperature sensing in hostile environments, Sens. Actuators A 237 (2016) 47–55. http://dx.doi.org/10.1016/j.sna.2015.11.012.

[3] J. Arajo, M. Mazo, A. Anta, P. Tabuada, K.H. Johansson, System architectures, protocols and algorithms for aperiodic wireless control systems, IEEE Trans. Ind. Inform. 10 (1) (2014) 175–184, doi:10.1109/TII.2013.2262281.

[4] E. Tanghe, W. Joseph, L. Verloock, L. Martens, H. Capoen, K.V. Herwegen, W. Vantomme, The industrial indoor channel: large-scale and temporal fading at 900, 2400, and 5200 mhz, IEEE Trans. Wireless Commun. 7 (2008) 2740–2751.

[5] P. Agrawal, A. Ahlén, T. Olofsson, M. Gidlund, Long term channel characterization for energy efficient transmission in industrial environments, IEEE Trans. Commun. 62 (8) (2014) 3004–3014, doi:10.1109/TCOMM.2014.2332876.

[6] O. Gnawali, R. Fonseca, K. Jamieson, D. Moss, P. Levis, Collection tree protocol, in: Proceedings of the 7th ACM Conference on Embedded Networked Sensor Systems, in: SenSys '09, ACM, New York, NY, USA, 2009, pp. 1–14, doi:10.1145/1644038.1644040.

[7] M. Sha, G. Hackmann, C. Lu, Arch: practical channel hopping for reliable home-area sensor networks, in: 2011 17th IEEE Real-Time and Embedded Technology and Applications Symposium, 2011, pp. 305–315, doi:10.1109/RTAS.2011.36.

[8] L.-O. Varga, M. Heusse, R. Guizzetti, A. Duda, Why is frequency channel diversity so beneficial in wireless sensor networks? IFIP Wireless Days, IFIP, Toulouse, France, 2016. URL https://hal.archives-ouvertes.fr/hal-01287518.

[9] F. Rezha, S.Y. Shin, Performance analysis of ISA100.11a under interference from an IEEE 802.11b wireless network, IEEE Trans. Ind. Inform. 10 (2) (2014) 919–927, doi:10.1109/TII.2014.2307016.

[10] D.S.J. De Couto, D. Aguayo, J. Bicket, R. Morris, A high-throughput path metric for multi-hop wireless routing, in: Proceedings of the 9th Annual International Conference on Mobile Computing and Networking, in: MobiCom '03, ACM, New York, NY, USA, 2003, pp. 134–146, doi:10.1145/938985.939000.

[11] R. Fonseca, O. Gnawali, K. Jamieson, P. Levis, Four-bit wireless link estimation, in: Proceedings of the Sixth ACM Workshop on Hot Topics in Networks (HotNets-VI), 2007.

[12] N. Baccour, A. Koubâa, H. Youssef, M. Alves, Reliable link quality estimation in low-power wireless networks and its impact on tree-routing, Ad Hoc Netw. 27 (2015) 1–25. http://dx.doi.org/10.1016/j.adhoc.2014.11.011.

[13] S. Rekik, N. Baccour, M. Jmaiel, K. Drira, Low-power link quality estimation in smart grid environments, in: Wireless Communications and Mobile Computing Conference (IWCMC), 2015 International, 2015, pp. 1211–1216, doi:10.1109/IWCMC.2015.7289255.

[14] F. Barac, S. Caiola, M. Gidlund, E. Sisinni, T. Zhang, Channel diagnostics for wireless sensor networks in harsh industrial environments, IEEE Sens. J. 14 (11) (2014a) 3983–3995, doi:10.1109/JSEN.2014.2356972.

[15] F. Barac, M. Gidlund, T. Zhang, Scrutinizing bit- and symbol-errors of IEEE 802.15.4 communication in industrial environments, IEEE Trans. Instrum. Meas. 63 (7) (2014b) 1783–1794, doi:10.1109/TIM.2013.2293235.

[16] R.D. Gomes, I.E. Fonseca, M.S. Alencar, Protocolos multicanais para redes de sensores sem fio industriais, Revista de Tecnologia da Informação e Comunicação 5 (2) (2015) 25–32.

[17] P. Agrawal, A. Ahlen, T. Olofsson, M. Gidlund, Characterization of long term channel variations in industrial wireless sensor networks, in: IEEE International Conference on Communications, 2014, pp. 1–6, doi:10.1109/ICC.2014.6883285.

[18] T. Olofsson, A. Ahln, M. Gidlund, Modeling of the fading statistics of wireless sensor network channels in industrial environments, IEEE Trans. Signal Process. 64 (12) (2016) 3021–3034, doi:10.1109/TSP.2016.2539142.

[19] P. Stenumgaard, J. Chilo, P. Ferrer-Coll, P. Angskog, Challenges and conditions for wireless machine-to-machine communications in industrial environments, IEEE Commun. Mag. 51 (6) (2013) 187–192, doi:10.1109/MCOM.2013.6525614.

[20] K.A. Remley, G. Koepke, C. Holloway, Camell, G. D., Measurements in harsh RF propagation environments to support performance evaluation of wireless sensor networks, Sens. Rev. 29 (2009) 211–222.

[21] M. Varela, M. Sanchez, Rms delay and coherence bandwidth measurements in indoor radio channels in the uhf band, IEEE Trans. on Vehicular Technology 50 (2001) 515–525.

[22] D.M. Amzucu, H. Li, E. Fledderus, Indoor radio propagation and interference in 2.4 GHz wireless sensor networks: Measurements and analysis, Wireless Pers. Commun. 76 (2014) 245–269.

[23] T. Watteyne, S. Lanzisera, A. Mehta, K.S.J. Pister, Mitigating multipath fading through channel hopping in wireless sensor networks, in: 2010 IEEE International Conference on Communications, 2010, pp. 1–5, doi:10.1109/ICC.2010.5502548.

[24] A. Gonga, O. Landsiedel, P. Soldati, M. Johansson, Revisiting multi-channel communication to mitigate interference and link dynamics in wireless sensor networks, in: 2012 IEEE 8th International Conference on Distributed Computing in Sensor Systems, 2012, pp. 186–193, doi:10.1109/DCOSS.2012.15.

[25] N. Baccour, A. Koubâa, L. Mottola, M.A. Zúñiga, H. Youssef, C.A. Boano, M. Alves, Radio link quality estimation in wireless sensor networks: a survey, ACM Trans. Sens. Netw. 8 (4) (2012) 34:1–34:33, doi:10.1145/2240116.2240123.

[26] L. Tang, K.-C. Wang, Y. Huang, F. Gu, Channel characterization and link quality assessment of IEEE 802.15.4-compliant radio for factory environments, IEEE Trans. Ind. Inform. 3 (2) (2007) 99–110, doi:10.1109/TII.2007.898414.

[27] W. Ikram, S. Petersen, P. Orten, N.F. Thornhill, Adaptive multi-channel transmission power control for industrial wireless instrumentation, IEEE Trans. Ind. Inform. 10 (2014) 978–990.

[28] C. Noda, S. Prabh, M. Alves, C.A. Boano, T. Voigt, Quantifying the channel quality for interference-aware wireless sensor networks, SIGBED Rev. 8 (4) (2011) 43–48, doi:10.1145/2095256.2095262.

[29] S. Zacharias, T. Newe, O. Sinead, E. Lewis, 2.4 GHz IEEE 802.15.4 channel interference classification algorithm running live on a sensor node, in: 2012 IEEE Sensors, 2012, pp. 1–4.

[30] Z. Jindong, W. Shuanhu, M. Chunxiao, F. Baode, L. Yunhong, Study and prediction of wireless link quality for adaptive channel hopping, J. Netw. 7 (11) (2012) 1884–1891.

[31] A. Bildea, O. Alphand, F. Rousseau, A. Duda, Link quality metrics in large scale indoor wireless sensor networks, in: IEEE 24th International Symposium on Personal, Indoor and Mobile Radio Communications, 2013, pp. 1888–1892.

[32] M. Eskola, T. Heikkil, Classification of radio channel disturbances for industrial wireless sensor networks, Ad Hoc Netw. 42 (2016) 19–33. http://dx.doi.org/10.1016/j.adhoc.2016.01.001.

[33] F. Entezami, M. Tunicliffe, C. Politis, Find the weakest link: statistical analysis on wireless sensor network link-quality metrics, IEEE Veh. Technol. Mag. 9 (3) (2014) 28–38, doi:10.1109/MVT.2014.2333693.

[34] C. Vallati, E. Ancillotti, R. Bruno, E. Mingozzi, G. Anastasi, Interplay of link quality estimation and RPLperformance: an experimental study, in: Proceedings of the 13th ACM Symposium on Performance Evaluation of Wireless Ad Hoc, Sensor, & Ubiquitous Networks, in: PE-WASUN '16, ACM, New York, NY, USA, 2016, pp. 83–90, doi:10.1145/2989293.2989299.

[35] V.C. Gungor, M.K. Korkmaz, Wireless link-quality estimation in smart grid environments, Int. J. Distrib. Sens. Netw. 8 (2) (2012) 214068, doi:10.1155/2012/214068.

[36] Z.Q. Guo, Q. Wang, M.H. Li, J. He, Fuzzy logic based multidimensional link quality estimation for multi-hop wireless sensor networks, IEEE Sens. J. 13 (10) (2013) 3605–3615, doi:10.1109/JSEN.2013.2272054.
[37] S. Rekik, N. Baccour, M. Jmaiel, K. Drira, Holistic link quality estimation-based routing metric for RPL networks in smart grids, in: 2016 IEEE 27th Annual International Symposium on Personal, Indoor, and Mobile Radio Communications (PIMRC), 2016, pp. 1–6, doi:10.1109/PIMRC.2016.7794925.
[38] M. Anwar, Y. Xia, Y. Zhan, Tdma-based IEEE 802.15.4 for low-latency deterministic control applications, IEEE Trans. Ind. Inform. 12 (1) (2016) 338–347, doi:10.1109/TII.2015.2508719.
[39] P. Bartolomeu, M. Alam, J. Ferreira, J. Fonseca, Survey on low power real-time wireless {MAC} protocols, J. Netw. Comput. Appl. 75 (2016) 293–316. http://dx.doi.org/10.1016/j.jnca.2016.09.004.
[40] D.D. Guglielmo, S. Brienza, G. Anastasi, {IEEE} 802.15.4E: a survey, Comput. Commun. 88 (2016) 1–24. http://dx.doi.org/10.1016/j.comcom.2016.05.004.
[41] R. Soua, P. Minet, Multichannel assignment protocols in wireless sensor networks: a comprehensive survey, Pervasive Mob. Comput. 16 (2015) 2–21.
[42] S. Petersen, S. Carlsen, Performance evaluation of wirelessHART for factory automation, in: IEEE Conference on Emerging Technologies & Factory Automation, 2009, pp. 1–9.
[43] W. Guo, W. Healy, M. Zhou, Impacts of 2.4-GHz ISM band interference on IEEE802.15.4 wireless sensor network reliability in buildings, IEEE Trans. Instrum. Meas. 61 (9) (2012) 2533–2544, doi:10.1109/TIM.2012.2188349.
[44] K. Benkic, M. Malajner, P. Planinsic, Z. Cucej, Using RSSI value for distance estimation in wireless sensor networks based on zigbee, in: 15th International Conference on Systems, Signals and Image Processing, 2008, pp. 303–306.
[45] K. Srinivasan, P. Dutta, A. Tavakoli, P. Levis, An empirical study of low-power wireless, ACM Trans. Sens. Netw. 6 (2) (2010) 16:1–16:49, doi:10.1145/1689239.1689246.
[46] J. Chilo, C. Karlsson, P. Angskog, P. Stenumgaard, Emi disruptive effect on wireless industrial communication systems in a paper plant, in: IEEE International Symposium on Electromagnetic Compatibility, 2009, pp. 221–224.
[47] J. Huang, G. Xing, G. Zhou, R. Zhou, Beyond co-existence: exploiting WiFi white space for zigBee performance assurance, in: Network Protocols (ICNP), 2010 18th IEEE International Conference on, 2010, pp. 305–314, doi:10.1109/ICNP.2010.5762779.
[48] V.C. Gungor, B. Lu, H.G. P., Opportunities and challenges of wireless sensor networks in smart grid, IEEE Trans. Ind. Electron. 57 (2010) 3557–3564.

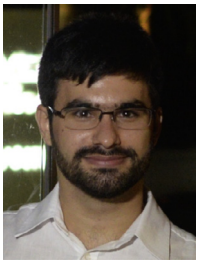

**Ruan D. Gomes** received his B.S. degree in Computer Science from Federal University of Paraíba, and his M.S. degree in Computer Science from Federal University of Campina Grande (UFCG). He currently works as a Lecturer at the Federal Institute of Education, Science, and Technology of Paraíba, Campus Guarabira. He is also a Ph.D. student in Electrical Engineering at UFCG, and is currently in a doctoral mobility at the Universidad Politécnica de Madrid. He has experience in R&D projects, mainly in the fields of embedded systems, wireless sensor networks, and multimedia systems.

**Diego V. Queiroz** received his B.Sc. in Computer Science at University Center of João Pessoa (2005) and B.Sc. in Technology of Computer Networks at Federal Institute of Education, Science and Technology of Paraíba (2008). He received his M.Sc. in Informatics from Federal University of Paraíba (UFPB) in 2015, and currently is a Ph.D student at Universidad Politécnica de Madrid. His research areas include: information security, computer networks, wireless communications and network simulators.

**Abel C. Lima Filho** received his B.Sc. Degree in Electrical Engineering, from Federal University of Campina Grande (UFCG), his M.Sc. and D.Sc. in Mechanical Engineering, from Federal University of Paraíba (UFPB), Brazil. He is currently a professor at the Mechanical Engineering Department of the Federal University of Paraíba.

**Iguatemi E. Fonseca** was born in Brazil, in 1974. He is currently an associate professor at the Informatics Center of the Federal University of Paraíba. He received the electronics engineering degree from the Federal University of Campina Grande (UFCG), Campina Grande, PB, Brazil, in 1999, and the M.Sc. and Ph.D degrees from the State University of Campinas (Unicamp), Campinas, SP, Brazil, in 2001 and 2005, respectively, specializing in nonlinear fiber optics and its applications, optical network design with physical-layer impairments and Impairment-Aware RWA. His current research interests include areas of the Electrical Engineering and Computer Science as: i) Communications Networks (Optical Networks, Wireless Sensor Networks, Mobile Networks and IP Networks), working on topics as identification/models of traffic in computer networks, techniques for identification and mitigation of denial of service attacks, algorithms and protocols in Industrial Wireless Sensor Networks, WDM and elastic optical networks with QoS requirements, and design and simulation of photonics devices; ii) Design of simulators in virtual reality with applications in industry sectors, as energy sector.

**Marcelo S. Alencar** was born in Serrita, Brazil in 1957. He received his Bachelor Degree in Electrical Engineering, from Universidade Federal de Pernambuco (UFPE), Brazil, 1980, his Master Degree from Universidade Federal da Paraíba (UFPB), Brazil, 1988 and his Ph.D from the University of Waterloo, Department of Electrical and Computer Engineering, Canada, 1994. Marcelo S. Alencar has more than 35 years of engineering experience, and 26 years as an IEEE Member, currently as Senior Member. For 18 years he worked for the Department of Electrical Engineering, Federal University of Paraíba, where he was Full Professor and supervised more than 50 graduate and several undergraduate students. Since 2003, he is Chair Professor at the Department of Electrical Engineering, Federal University of Campina Grande, Brazil. He published 20 books and more than 420 papers in journals and conferences. He is columnist of the traditional newspaper Jornal do Commercio, in Recife, Brazil.